Synthesis of oligo(*p*-phenylene)-linked dyads containing free base, zinc(II) or thallium(III) porphyrins for studies in artificial photosynthesis

Masahiko Taniguchi, Jonathan S. Lindsey *

Department of Chemistry, North Carolina State University, Box 8204, Raleigh, NC 27695-8204, USA

ARTICLE INFO

ABSTRACT

A series of (*p*-phenylene)$_n$-linked *meso*-mesityl-substituted porphyrin dyads (*n*=2–4) was prepared via Suzuki coupling of zinc(II) and free base porphyrin building blocks. The resulting zinc(II)/free base porphyrin dyads were demetalated. The series of free base porphyrin dimers (*n*=1–4), four other porphyrin dimers (with *p*-phenylene, diphenylethyne or diphenylbutadiyne linkers; and aryl or tridec-7-yl *meso* substituents), and several benchmark monomers were converted to the thallium(III)chloride complexes under mild conditions. The collection of eight Tl(III)Cl/Tl(III)Cl dimers is designed for studies of ground-state hole-transfer processes and comparison with the excited-state energy- and hole-transfer processes of the corresponding Zn(II)/free base dyads. Altogether, 18 new porphyrin arrays and benchmark monomers have been prepared.

1. Introduction

One of the key objectives in artificial photosynthesis is to gain a deep understanding of the physical principles that underlie light-harvesting and energy-transduction processes. The processes of interest include excited-state energy-transfer (as occurs in the photosynthetic antenna complexes), excited-state electron-transfer (as occurs in the reaction center), and subsequent ground-state hole- and electron-transfer reactions that give rise to a spatially separated hole and electron of sufficient lifetime for ultimate storage of energy in the form of chemical fuels.

Studies to examine electronic communication among interacting constituents have focused on multiporphyrin arrays wherein the porphyrins serve as surrogates for the naturally occurring (bacterio)chlorophylls, and the linker that joins the porphyrins provides for architectural control in lieu of a protein matrix. A vast number of synthetic arrays have been prepared to date.[1–14] Still, there remains a need for arrays with systematic variation of the

parameter under investigation, such as distance, orientation, energetics, frontier-orbital composition, excited-state lifetime, π-framework (e.g., hydroporphyrin vs porphyrin), etc. Our goal was to create a set of arrays to enable direct comparison of processes of (1) excited-state energy transfer in neutral complexes, (2) excited-state hole transfer in singly oxidized complexes, and (3) ground-state hole-transfer in singly oxidized complexes, all as a function of increasing linker length between two interacting porphyrins. The collective studies were aimed to deepen our understanding of electronic communication between the porphyrins, largely mediated by the intervening linker that supports such processes.

To achieve this goal we sought a specific set of compounds wherein two porphyrins of distinct or identical metalation states were joined at the *meso*-positions via a relatively rigid linker of defined distance (Chart 1). The metalation states included zinc(II)/free base ('ZnFb') for excited-state energy-transfer and hole-transfer studies, and thallium(III)/thallium(III) ('TlTl') for ground-state hole-transfer studies. Diverse ZnFb porphyrin dyads have been prepared with linkers of a range of lengths,[6] but to our knowledge, no Tl(III)-containing porphyrin arrays of any type have heretofore been prepared. For our studies, the primary linker of choice was an oligo(*p*-phenylene) unit to achieve a high degree of

* Corresponding author. Tel.: +1 9195156406; fax: +1 9195132830; e-mail address: jlindsey@ncsu.edu (J.S. Lindsey).

molecular rigidity and substantial increments of distance (phenyl—quaterphenyl) within a given molecular composition. Two other linkers (diphenylethyne, diphenylbutadiyne) were employed for comparison with the large body of available data concerning multiporphyrin arrays of these types.[7]
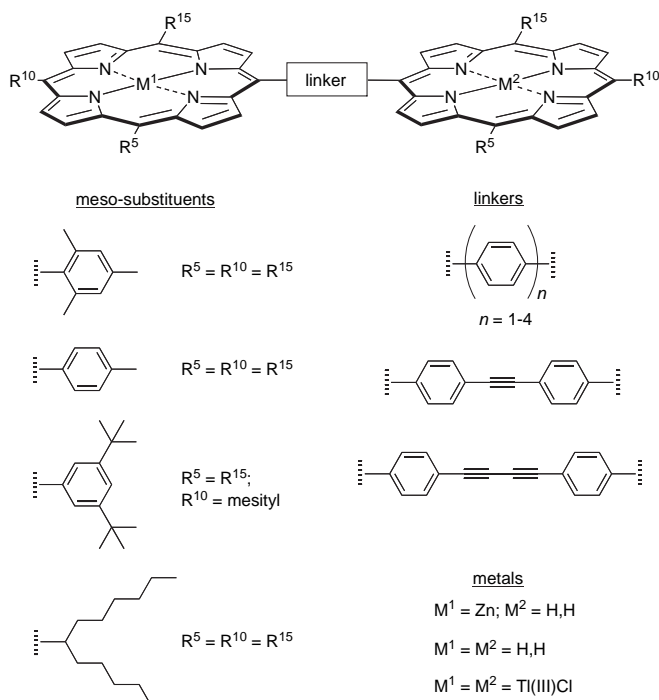

meso-substituents

$R^5 = R^{10} = R^{15}$

$R^5 = R^{10} = R^{15}$

$R^5 = R^{15}$;
R^{10} = mesityl

$R^5 = R^{10} = R^{15}$

linkers

n = 1–4

metals

M^1 = Zn; M^2 = H,H

$M^1 = M^2$ = H,H

$M^1 = M^2$ = Tl(III)Cl

Chart 1.

Key molecular design issues in addition to the linker included the following: (i) pattern of substitution of the non-linking substituents, (ii) electronic features of the non-linking substituents, and (iii) solubilizing features of the non-linking substituents.[7] Porphyrins bearing electron-releasing aryl groups (e.g., phenyl) or alkyl groups located at the *meso*-positions typically exhibit the a_{2u} HOMO (vs a_{1u} HOMO with β-alkyl or *meso*-pentafluorophenyl-substituted porphyrins). The a_{2u} orbital is desired owing to the large electron density at the *meso*-position, the site where the oligo(*p*-phenylene) linker is positioned. Accordingly, a bulky, electron-rich group was located at each of the non-linking *meso*-positions to achieve the desired frontier-orbital composition and a high degree of solubilization in organic solvents.

In this paper we report the synthesis of 18 new porphyrin arrays and benchmark compounds. The primary targets included the arrays containing two porphyrins linked by oligo-*p*-phenylene units (spanning phenyl—quaterphenyl), mesityl groups at the non-linking *meso* sites, and several distinct metalation states (FbFb, ZnFb, and TlTl). Four TlTl dimers equipped with various non-linking substituents (mesityl, 3,5-di-*tert*-butylphenyl, tridec-7-yl) and linkers (*p*-phenylene, diphenylethyne, diphenylbutadiyne) also were prepared. Of this latter set, three of the constructs were previously known as the FbFb species and were subjected here to metalation, whereas the swallowtail-substituted diphenylethyne-linked FbFb dimer was prepared herein from the corresponding building blocks. Altogether, three new ZnFb porphyrin dyads, three new FbFb porphyrin dimers, eight new TlTl porphyrin dimers, and four thallium-containing porphyrin monomers are described herein. The photochemical features of the ZnFb porphyrin dyads were recently described,[15,16] whereas the ground-state hole-transfer properties of the TlTl porphyrin dimers will be described elsewhere.

2. Routes to oligo(*p*-phenylene)-linked porphyrin dyads

Synthetic oligo(*p*-phenylene)-linked porphyrin dyads have been prepared via a wide variety of chemistries. The various approaches can be assessed on the basis of (i) whether the route provides rational access to (symmetric) dimers or (unsymmetric) dyads, and (ii) at what stage in the synthesis the porphyrin macrocycle is constructed. In this regard, the oligo(*p*-phenylene) linker can be pre-installed on an acyclic precursor to the porphyrin followed by a cyclization reaction to create the porphyrin macrocycle, or intact porphyrin building blocks can be joined via Suzuki coupling to form the oligo(*p*-phenylene) linker. The Suzuki coupling can entail a single joining (mono-coupling) to create dyads or a double joining (bis-coupling) to create dimers. In general, any route to dyads can be employed to access dimers. Representative routes are displayed in Table 1.
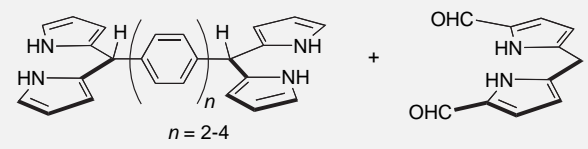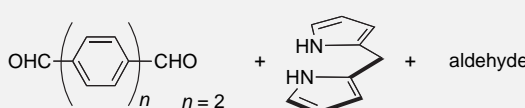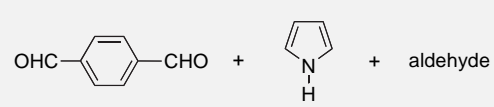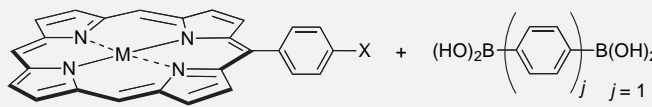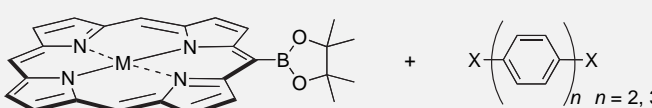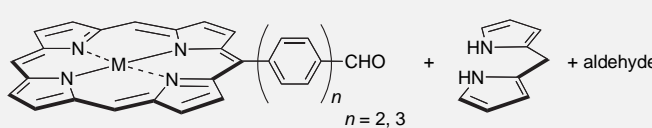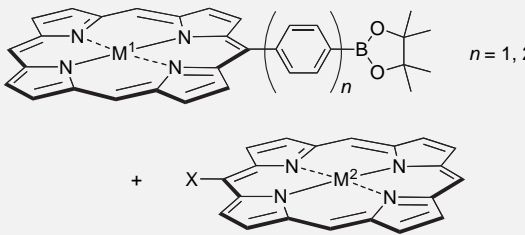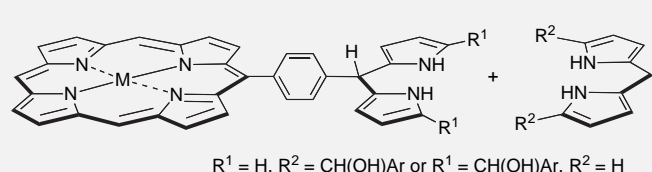
Synthesis of a biphenyl-linked porphyrin dimer was first reported by McLendon and co-workers, via condensation of a 4,4′-biphenyl-linked bis(dipyrromethane) and a 1,9-diformyldipyrro-methane followed by oxidation (entry 1).[17,18] Extension of this method with a 4,4″-terphenyl- or 4,4‴-quaterphenyl-linked bis(dipyrromethane) afforded terphenyl- or quaterphenyl-linked porphyrin dimers.[19] Alternatively, the reaction of biphenyl-4,4′-dicarboxaldehyde, a dipyrromethane and an aldehyde gave a symmetric biphenyl-linked porphyrin dimer (entry 2).[20–22] Similar reaction of terephthalaldehyde, benzaldehyde, and pyrrole afforded the *p*-phenylene-linked dimer (entry 3).[23,24] This reaction is statistical in that multiple porphyrin products can form, and is undirected in that no control is provided over the individual metalation state of each porphyrin.

The Suzuki coupling reaction enables C—C bond formation to create the oligo(*p*-phenylene) linkers, which gives strategic flexibility in the preparation of oligo(*p*-phenylene)-linked porphyrin arrays. Biphenyl- and terphenyl-linked porphyrin dimers were prepared by Suzuki coupling of a halophenylporphyrin and a linker bearing a bis(boronic acid) unit (entry 4).[25,26] Similar Suzuki coupling was employed with a *meso*-substituted dioxaborolanylporphyrin and a dihalo-substituted phenylene linker (entry 5).[27] Both examples provide rational access to dimers yet were undirected with respect to the metalation states and substituents of the respective porphyrins.

The synthesis of dyads requires a directed route wherein the two porphyrins are created sequentially, or two porphyrin building blocks are joined in an unsymmetric fashion. The condensation of a porphyrin bearing a *p*-biphenylcarboxaldehyde unit with a dipyr-romethane and an aldehyde gave the biphenyl-linked porphyrin dyad (entry 6).[28,29] This approach was statistical in that a porphyrin triad and a porphyrin monomer also could form. We reported the Suzuki mono-coupling of a dioxaborolanylphenylporphyrin and a *meso*-haloporphyrin; although the synthesis was rational and entailed a directed coupling, the product was a *p*-phenylene-linked porphyrin dimer rather than a dyad given that both porphyrins contained the same substituents and were free base species (entry 7).[30] Nocera and co-workers recently reported the Suzuki mono-coupling of a dioxaborolanylbiphenylporphyrin and a *meso*-halo-porphyrin to give a biphenyl-linked porphyrin dyad (entry 7).[31] Following these approaches, porphyrin dyads bearing linkers as long as the quaterphenyl unit have been reported so far.[18]

The reaction of a porphyrin bearing a dipyrromethane with a dipyrromethane/dicarbinol (or vice versa) afforded the corresponding *p*-phenylene-linked porphyrin dyad (entry 8).[32] The porphyrin-forming conditions were sufficiently mild to accommodate metalation states such as Zn/Fb, Mg/Fb, and Zn/Mg. Porphyrin dyads in distinct metalation states (e.g., ZnFb) in principle can be prepared by statistical metalation or demetalation of porphyrin dimers. In practice, however, separation of zinc/zinc, zinc/free base, and free base/free base arrays typically entails elaborate chromatography.

Table 1
Routes to oligo(p-phenylene)-linked porphyrin dimers and dyads

Entry	Reactants	Joining Reaction	n^b	Type	Architecture	References
1		Porphyrin formation	2–4	Rational, undirected	Dimer	17–19
2		Porphyrin formation	2	Statistical, undirected	Dimer	20–22
3		Porphyrin formation	1	Statistical, undirected	Dimer	23,24
4[a]		Suzuki bis-coupling	3	Rational, undirected	Dimer	25,26
5[a]		Suzuki bis-coupling	2,3	Rational, undirected	Dimer	27
6[a]		Porphyrin formation	2,3	Statistical, directed	Dyad	28,29
7[a]		Suzuki mono-coupling	1,2	Rational, directed	Dyad	30,31
8[a]		Porphyrin formation	1	Rational, directed	Dyad	32

[a] Substituents on the porphyrin macrocycle are not shown for clarity.
[b] Number of p-phenylene units in the oligo(p-phenylene) linker.

3. Results and discussion

3.1. Synthesis of oligo(p-phenylene)-linked porphyrin dyads and dimers

To achieve a rational, directed synthesis of oligo(p-phenylene)-linked porphyrin dyads, we chose the Suzuki mono-coupling of a zinc porphyrin and a free base porphyrin, as in entry 7 of Table 1.

To minimize the number of reaction steps, meso-phenyl and meso-biphenyl-substituted porphyrins were prepared, instead of meso-halo or meso-pinacolatoboron-substituted porphyrins, which require additional steps for halogenation and introduction of the pinacolatoboron unit. The choice of mesityl groups at the non-linking positions to impart solubility requires use of mixed-aldehyde condensations to prepare the A₃B-porphyrin building blocks, because trimesitylporphyrins cannot yet be prepared in a rational

Scheme 1.
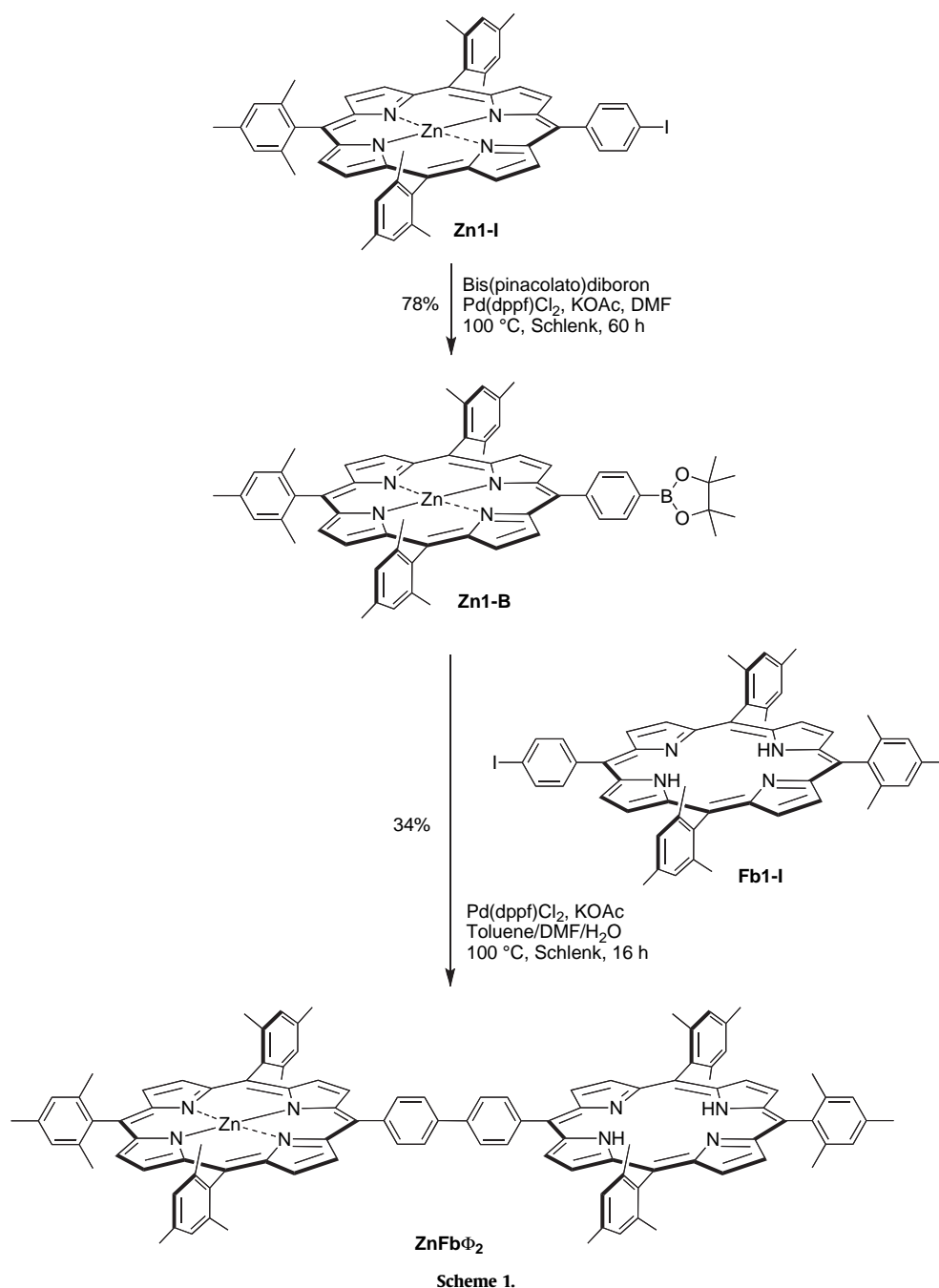
manner.[33] Thus, all trimesityl-substituted porphyrin building blocks were synthesized via statistical condensations[34] of pyrrole, mesitaldehyde, and a second aldehyde in the presence of $BF_3 \cdot O(Et)_2$/ethanol cocatalysis.[35]

The synthesis of biphenyl-linked porphyrin dyad **ZnFbΦ₂** is outlined in Scheme 1. Pd-mediated coupling of known[36] iodophenyl-substituted zinc porphyrin **Zn1-I** with bis(pinacolato)diboron gave *meso*-dioxaborolanylphenylporphyrin **Zn1-B** in 78% yield. Suzuki coupling of **Zn1-B** and known[34] iodophenyl-substituted free base porphyrin **Fb1-I** was carried out in toluene/DMF/water containing 1,1′-bis(diphenylphosphino)ferrocene-palladium(II)dichloride dichloromethane adduct and potassium acetate. In general, the purification of multiporphyrin arrays formed upon Pd-mediated coupling is typically best achieved via a multi-column chromatographic sequence: (1) silica chromatography to remove palladium species and other polar materials; (2)

preparative-scale size-exclusion chromatography (SEC) to separate the target array from monomers and higher-molecular weight materials (e.g., oligomers); and (3) silica to remove materials derived from the SEC column.[36] In some cases here, the first silica column was omitted. Thus, treatment of the crude mixture in this manner afforded biphenyl-linked porphyrin dyad **ZnFbΦ₂** in 34% yield.

The synthesis of the biphenyl-substituted porphyrin building blocks requires access to bifunctionalized biphenyl units. Thus, monoformylation of 4,4′-dibromobiphenyl with *n*-BuLi and DMF following a known procedure[37] gave aldehyde **I-Br** (Scheme 2). Pd-mediated reaction of **I-Br** and bis(pinacolato)diboron gave known aldehyde **I-B**.[38] A mixed condensation was performed of 2.5 mM of biphenylcarboxaldehyde **I-Br** or **I-B**, 7.5 mM of mesitaldehyde, and 10 mM of pyrrole. The reaction was carried out in $CHCl_3$ (containing 0.8% ethanol)[35] in the presence of 3 mM $BF_3 \cdot O(Et)_2$
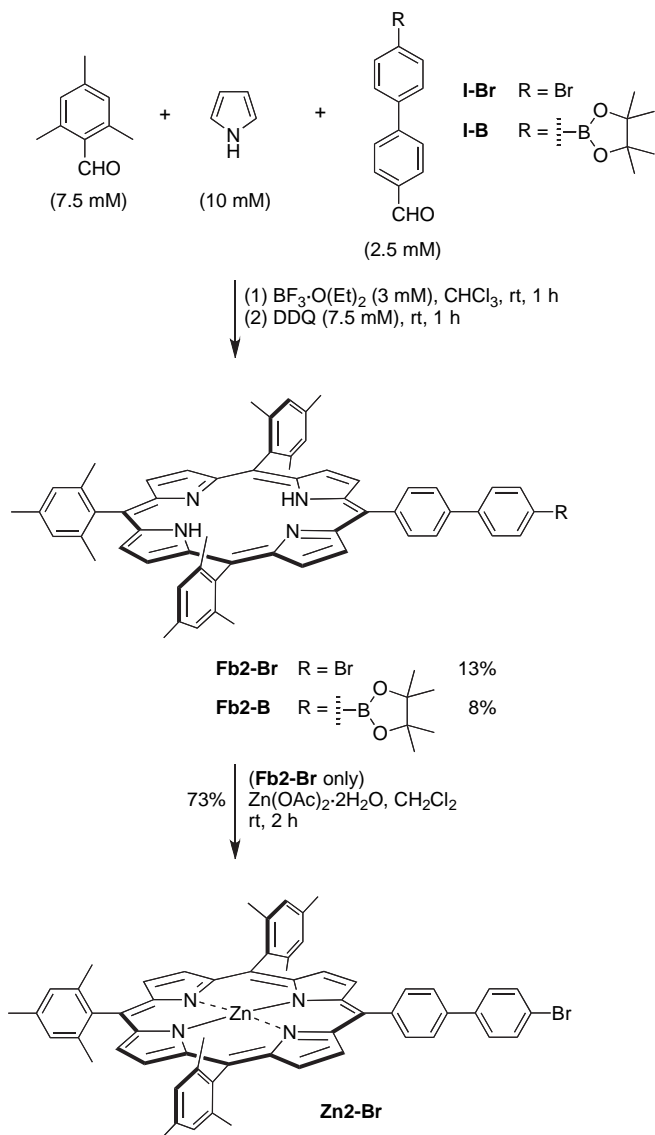
Scheme 2.

for 1 h, followed by oxidation with DDQ to form the mixture of porphyrins. Chromatography of the crude reaction mixture readily gave the desired A₃B-porphyrin **Fb2**-**Br** or **Fb2**-**B** in 13 or 8% yield, respectively, which is comparable to the typical yield of A₃B-porphyrins via mixed-aldehyde condensations (10–14%).[34] Treatment of **Fb2**-**Br** with $Zn(OAc)_2 \cdot 2H_2O$ in CH_2Cl_2 at room temperature gave **Zn2**-**Br** in 73% yield. For comparison, an analogous *meso*-biphenyl-substituted porphyrin was prepared by two Suzuki coupling procedures: (1) chemoselective Suzuki mono-coupling of a *meso*-(dioxaborolanylphenyl)porphyrin and 4-iodo-1-chlorobenzene, (2) Suzuki bis-coupling of the resulting *meso*-(*p*-chlorobiphenyl)porphyrin and bis(pinacolato)diboron.[31]

Terphenyl- and quaterphenyl-linked porphyrin dyads were synthesized via Suzuki coupling of the corresponding building blocks in a manner similar to that employed in the synthesis of **ZnFbΦ₂** (Scheme 3). Suzuki coupling of dioxaborolanylphenylporphyrin **Zn1**-**B** and bromobiphenylporphyrin **Fb2**-**Br** gave terphenyl-linked porphyrin dyad **ZnFbΦ₃** in 58% yield, whereas bromobiphenylporphyrin **Zn2**-**Br** and dioxaborolanylbiphenylporphyrin **Fb2**-**B** gave quaterphenyl-linked porphyrin dyad **ZnFbΦ₄** in 63% yield. These reactions were carried out at a scale that gave dyads in quantities of up to 50 mg.

Oligo(*p*-phenylene)-linked free base porphyrin dimers were prepared via demetalation of zinc-free base dyads containing the biphenyl, terphenyl, or quaterphenyl linker to give porphyrin dimers **FbFbΦ₂**, **FbFbΦ₃**, or **FbFbΦ₄**, respectively (Scheme 4). The *p*-phenylene-linked porphyrin dimer **FbFbΦ** was previously prepared by mixed condensation of mesitaldehyde, pyrrole, and terephthalaldehyde, and **ZnFbΦ** was prepared therefrom by statistical metalation.[24] The excited-state processes for **ZnFbΦ** in the respective neutral[24] and oxidized[15] form have been characterized.

3.2. Synthesis of a swallowtail-substituted porphyrin dimer

The Sonogashira coupling of swallowtail-substituted porphyrin building blocks was employed to prepare the corresponding diphenylethyne-linked swallowtail porphyrin dimer. The swallowtail substituents have previously been employed to impart high solubility to porphyrins and multiporphyrin arrays in organic solvents.[39,40] Thus, the known free base swallowtail porphyrins[39] bearing ethynyl (**Fb4**-**E**) and iodo (**Fb4**-**I**) groups were coupled under copper-free, palladium-mediated coupling conditions[41,42] to afford the diphenylethyne-linked dimer **FbFb-SW-PEP** in 48% yield (Scheme 5).

3.3. Synthesis of thallium(III) complexes of porphyrins

3.3.1. Prior metalation conditions. The first report concerning the synthesis of a thallium porphyrin apparently was due to Fischer, while the modern era began with the work of Smith.[43] Smith prepared thallium(III) chelates of 2,3,7,8,12,13,17,18-octaethylporphyrin, *meso*-tetraphenylporphyrin, and several derivatives of naturally occurring porphyrins; subsequent characterization methods included absorption, IR, and ¹H NMR spectroscopy.[43] He also reported ¹³C NMR spectra of selected thallium(III) porphyrins.[44] Thallium(III) porphyrins are class II metalloporphyrins, which characteristically resist demetalation except under quite acidic conditions (conc. H_2SO_4 at room temperature),[45] although reducing agents that give the Tl(I) species enable milder demetalation.[43] The traditional methods for thallium(III) chelation include treating the free base porphyrin with a thallium salt in refluxing pyridine or refluxing DMF;[45] however, Smith employed $Tl(O_2CCF_3)_3$ in a solvent mixture (THF and CH_2Cl_2) that was warmed slightly or at room temperature.[43] This extensive prior work provided the foundation for the following studies concerning the metalation of various porphyrin dimers.

3.3.2. Metalation conditions for diverse synthetic porphyrins. The studies of ground-state hole transfer in the TlTl dimers require the presence of identical counterions at the two metal centers, and are best performed with chloride counterions. The reaction of a free base porphyrin and $TlCl_3 \cdot (H_2O)_4$ in DMF under reflux affords the thallium(III) complex wherein the apical ligand typically is chloride.[46] Alternatively, a thallium(III) complex wherein the apical ligand is acetate or trifluoroacetate can be subjected to exchange to form the chlorothallium(III) complex.[47–52] The reaction of free base *meso*-tetramesitylporphyrin (**Fb-TMP**) with $TlCl_3 \cdot (H_2O)_4$ in DMF at 150 °C for 2 h afforded the thallium complex **Tl-TMP** bearing chloride as the apical ligand. However, thallium metalation of swallowtail porphyrin dimer **FbFb-SW-PEP** with $TlCl_3 \cdot (H_2O)_4$ in DMF at 150 °C resulted in decomposition within 30 min. Thus, reactions under milder conditions were explored.

We found that the reaction of free base porphyrins with a methanolic solution of $TlCl_3 \cdot (H_2O)_4$ in CH_2Cl_2 at room temperature proceeds smoothly; the reaction mixture quickly turns (within 1 min) from purple to green. The formation of the thallium porphyrin can be readily monitored by absorption spectroscopy (vide infra) and by TLC, which imply that >90% of the free base porphyrin is converted to the corresponding thallium porphyrin within 1 h. These room temperature conditions for thallium metalation are
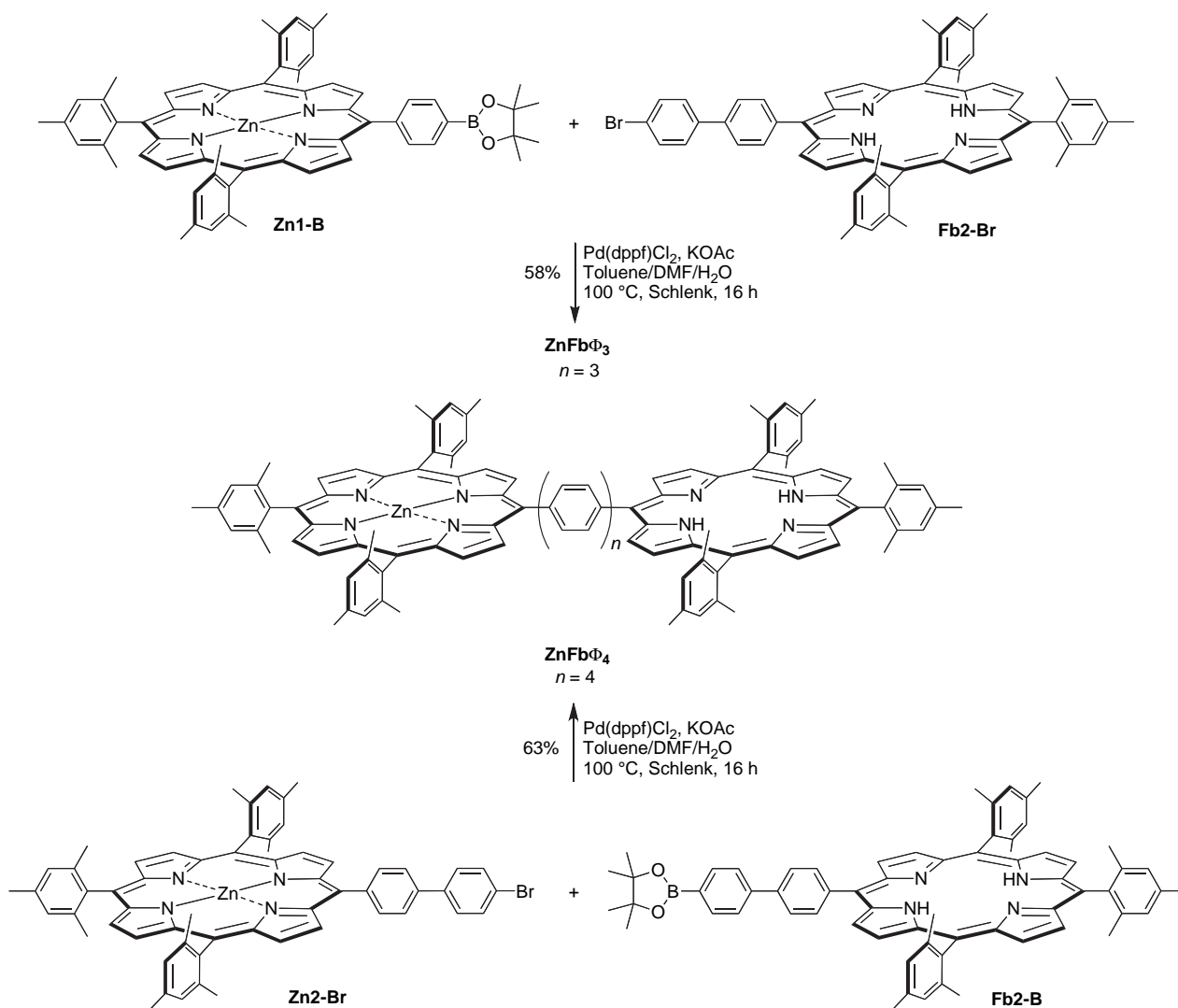
Scheme 3.

mild and quite attractive in affording conversion of 90% or greater; however, the reaction is typically not fully complete. Achieving high purity is essential for photochemical studies.

We found the full conversion to the thallium chelate could not be achieved despite (1) prolonged reaction time (up to 72 h), (2) use of a large excess of $TlCl_3 \cdot (H_2O)_4$ (up to 200 equiv), and (3) use of higher temperature (e.g., in THF at reflux; in DMF at 150 °C). As a result, purification of the thallium complex from the unreacted free base porphyrin (up to 5%) is required. Whereas the thallium porphyrin monomers can be readily purified by chromatography (silica or neutral alumina) to remove the unreacted free base porphyrin, purification of the TlTl porphyrin dimer from a trace amount of the Tl/Fb porphyrin dyad and starting material required extensive chromatography. Alternatively, the thallium porphyrin species (monomers and dimers) could be recrystallized upon diffusion of methanol (or hexanes) into a chloroform solution of the mixture of porphyrins. Application of such chromatographic or crystallization methods afforded the requisite purity in each case.

The reaction conditions applied for thallium metalation and the yields obtained are summarized in Table 2. The thallium(III) porphyrin monomers that were prepared herein are illustrated in Chart 2. The thallium porphyrins **Tl1-E** and **Tl4-E** were prepared (by metalation of the free base species **Fb1-E** and **Fb4-E**) as benchmark compounds for comparison with the analogous dimers.

Thallium porphyrin **Tl3-OH** (prepared from known[53] **Fb3-OH**) bears a hydroxymethyl group for surface attachment.

The thallium(III) complexes of the porphyrin dimers that were prepared herein are shown in Chart 3. The dimers wherein the linker varies in length and composition include the oligo-(p-phenylene)-linked architectures as well as those containing the diphenylethyne (**TlTl-PEP**) and diphenylbutadiyne (**TlTl-PEEP**) linkers. The latter arrays were obtained by metalation of the known free base architectures (**FbFb-PEP**,[54] **FbFb-PEEP**[41]). To study the effect of *meso* substituents, known[30] p-phenylene-linked dimer **FbFb-Ar-Φ** and the new diphenylethyne-linked swallowtail dimer **FbFb-SW-PEP** were converted to the corresponding thallium complexes **TlTl-Ar-Φ** and **TlTl-SW-PEP**. All thallium porphyrins described herein were analyzed by fluorescence emission and excitation spectroscopy to verify that the samples were devoid of free base porphyrins. MALDI-MS analysis of the thallium porphyrins typically exhibited two dominant peaks in the positive ion spectrum including the molecule ion and a daughter ion formed upon loss of chloride.

3.4. Characterization of synthetic porphyrins and arrays

All porphyrin monomers, dimers (FbFb, TlTl), and dyads (ZnFb) were characterized by ^1H NMR spectroscopy, absorption spectroscopy, emission spectroscopy, laser-desorption mass spectrometry
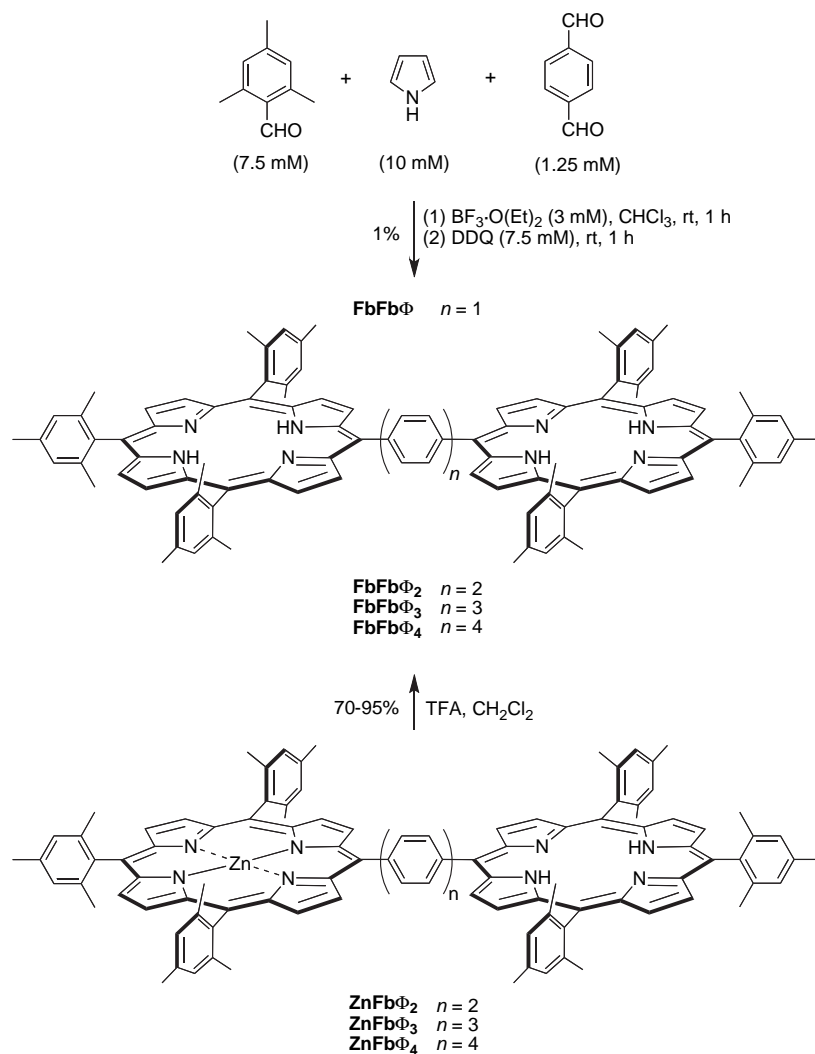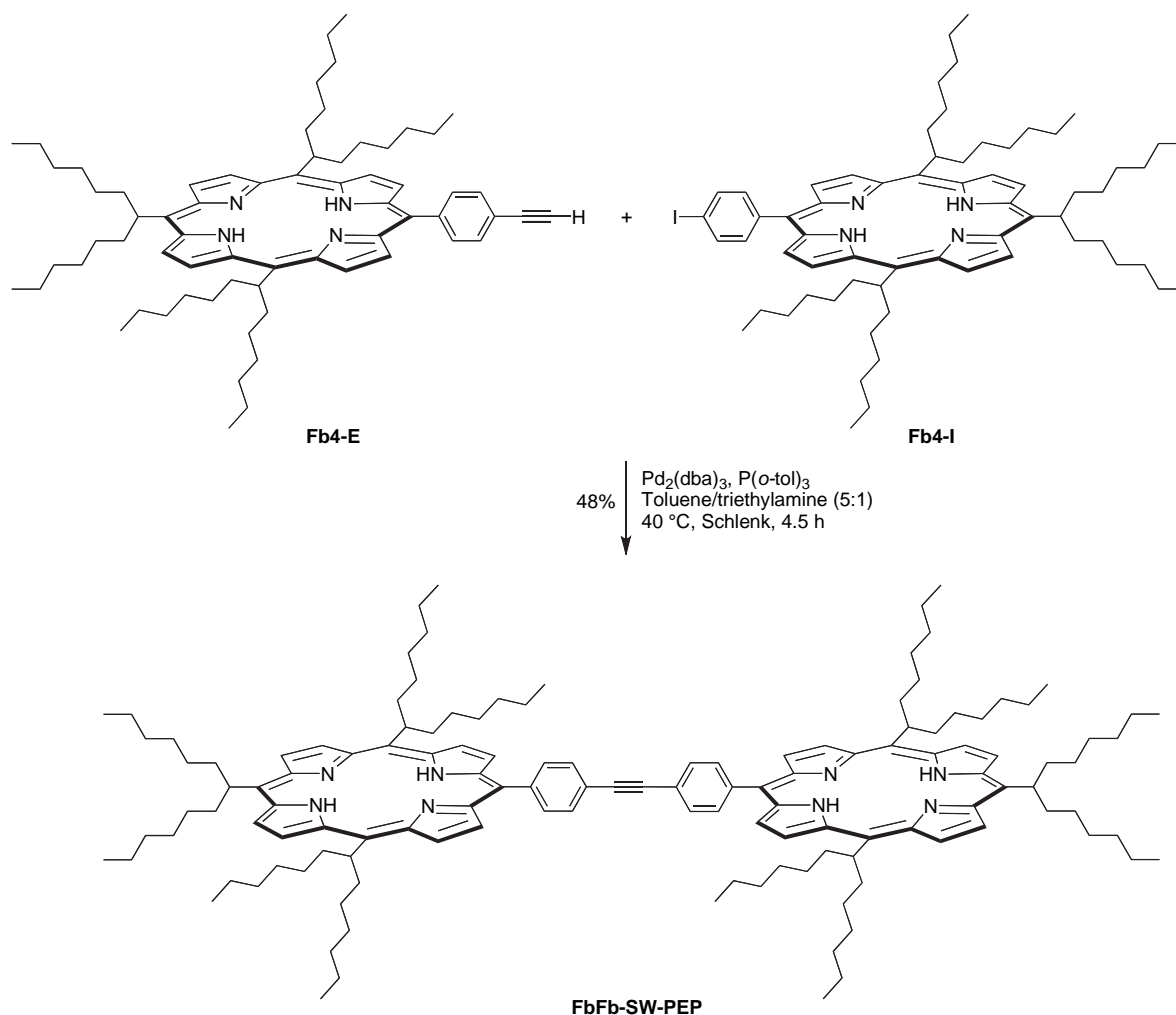
Scheme 4.

(low resolution), electrospray mass spectrometry (high resolution), and analytical SEC (vide infra). The characterization of the arrays by ^{13}C NMR spectroscopy proved difficult owing to very low solubility for the FbFb dimers, complexity of the spectra for the ZnFb dyads (composed of two distinct A3B-porphyrins), and strong Tl–C couplings in the TlTl dimers. The NMR spectral features of the porphyrin monomers, dimers, and dyads are described below.

3.4.1. Size-exclusion chromatography. Analytical size-exclusion chromatography (SEC) has served as an effective means of establishing the purity of diverse covalently linked multiporphyrin arrays.[36,41,42,55] A very attractive feature of SEC is that because the mode of separation relies on differences in molecular size rather than adsorption, essentially all of the material injected into the column elutes from the column. Each of the new purified oligo(*p*-phenylene)-linked arrays was examined by analytical SEC with visible-region absorption spectroscopic detection. Each compound gave a single peak, as expected, upon SEC analysis (Fig. 1). The retention time for an array with a given linker was essentially constant regardless of metalation state (Table 3). Moreover, the retention time decreased by ∼0.4 min per additional *p*-phenylene unit regardless of metalation state. Accordingly, the existence of a single peak for each array is indicative of sample purity. The data listed in Table 3 are for the arrays with increasing number of *p*-phenylene units. The swallowtail dimer also gave a single peak

distinct from that of the monomer upon analytical SEC, consistent with the dimer architecture.

3.4.2. NMR spectra of thallium porphyrins. To our knowledge, the only thallium complexes of *meso*-substituted porphyrins that have been characterized by ^{1}H NMR and ^{13}C NMR spectroscopy are symmetric A4-porphyrins (i.e., bearing four identical *meso*-substituents).[52,56–61] The ^{1}H and ^{13}C NMR spectra obtained herein of a thallium complex of an A4-porphyrin, namely **Tl-TMP**, are very similar to those previously reported for thallium complexes of A4-porphyrins. Due to the strong thallium-proton and thallium-carbon couplings, the following characteristic patterns were observed: (1) ^{1}H NMR spectra; (a) the β-protons show strong ^4J couplings (62.4 Hz) with thallium, (b) the *o*-/*o*′-methyl and *m*-/*m*′-H in the mesityl group are differentiated due to the presence of the axial ligand. (2) ^{13}C NMR spectra; (a) the magnitude of the coupling constants between carbon and thallium decreases in the following order: *meso*-porphyrin carbon (^3J, 146 Hz)>β-porphyrin carbon (^3J, 116 Hz)>>*o*-mesityl carbon (^4J, 26 Hz)>*m*-mesityl carbon (^5J, 19 Hz)=α-porphyrin carbon (^2J, 19 Hz), (b) in addition to the Tl–C coupling, the *o*-/*o*′- and *m*-/*m*′-mesityl carbons are differentiated due to the presence of the axial ligand; thus, the *o*-mesityl carbon affords a doublet of doublets pattern.

The effects of thallium on the ^{13}C NMR spectra are best illustrated by comparison of the ^{13}C NMR spectra in the series of

Scheme 5.

meso-tetramesitylporphyrin species including the free base (**Fb-TMP**), zinc chelate (**Zn-TMP**),[62] and chlorothallium derivative (**Tl-TMP**). The spectra are displayed in Figure 2. Each of the porphyrins is of the A_4-type, and in each case all of the observed signals are readily assignable. Note that the signal for the porphyrin α-carbon of **Fb-TMP** is missing (owing in part to NH tautomerization) under the spectroscopic conditions employed.

The NMR spectra of thallium A_3B-porphyrins are more complicated due to the decreased symmetry (vs the A_4-porphyrins) of the porphyrin macrocycle. For instance, the ^1H NMR spectrum of A_3B-porphyrin **Tl1-E** exhibits four sets of inequivalent β-porphyrin

protons. Out of four sets of inequivalent β-porphyrin protons (total 8H), two sets of β-porphyrin protons adjacent to two mesityl groups (4H) are overlapped and appear as a doublet [^4J(Tl–H)= 62.0 Hz] (note that ^3J(H–H) are not observed). Each of the remaining two sets of β-porphyrin protons (4H) appears as a doublet of doublets [^4J(Tl–H)=62.8 Hz, ^3J(H–H)=4.7 Hz] and [^4J(Tl–H)=64.5 Hz, ^3J(H–H)=4.7 Hz]. The ^1H NMR spectra of thallium porphyrin dimers are essentially the superposition of the spectra of the constituent thallium A_3B-porphyrins.

The ^{13}C NMR spectra of thallium-containing A_3B-porphyrins and TlTl dimers (which contain two identical A_3B-porphyrins) show typical patterns for coupling between carbon and thallium as seen for A_4-porphyrins. However, the assignment and interpretation of the resonances are complicated due to the decreased symmetry of the porphyrin macrocycle and the strong thallium/carbon coupling, whereas the signal-to-noise is limited owing to available quantity of the sample. Representative ^{13}C NMR spectra of one Tl-porphyrin monomer and five TlTl dimers are shown in Figure 3. ^{13}C NMR spectra of seven such compounds are provided without assignments as Supplementary data.

3.4.3. Absorption spectra of thallium(III) porphyrins. The absorption spectra of the thallium(III) porphyrins are summarized in Table 4. Representative spectra of thallium(III) complexes of porphyrin dimers and the corresponding free base porphyrins (**FbFbΦ₄**, **TlTl-Φ₄**, **FbFbΦ**, and **TlTl-Φ**) are displayed in Figure 4. The absorption spectra of thallium(III) porphyrins show patterns typical for

Table 2
Synthesis of thallium(III) complexes of porphyrins and porphyrin dimers

| Free base porphyrin	Thallium chelate	Solvent	Temp (°C)	Time (h)	Yield (%)
Fb-TMP	**Tl-TMP**	DMF	150	2	75
Fb1-E	**Tl1-E**	CH_2Cl_2/CH_3OH	rt	0.5	90
Fb3-OH	**Tl3-OH**	CH_2Cl_2/CH_3OH	rt	48	78
Fb4-E	**Tl4-E**	CH_2Cl_2/CH_3OH	rt	2	63
FbFb-Ar-Φ	**TlTl-Ar-Φ**	DMF	150	2	75
FbFb-Φ	**TlTl-Φ**	CH_2Cl_2/CH_3OH	rt	2	80
FbFb-Φ₂	**TlTl-Φ₂**	CH_2Cl_2/CH_3OH	rt	2	83
FbFb-Φ₃	**TlTl-Φ₃**	CH_2Cl_2/CH_3OH	rt	14	84
FbFb-Φ₄	**TlTl-Φ₄**	CH_2Cl_2/CH_3OH	rt	2	78
FbFb-PEP	**TlTl-PEP**	CH_2Cl_2/CH_3OH	rt	16	71
FbFb-PEEP	**TlTl-PEEP**	$CHCl_3/CH_3OH$	60	1.5	66
FbFb-SW-PEP	**TlTl-SW-PEP**	CH_2Cl_2/CH_3OH	rt	2	76

Tl-TMP

Tl1-E

Tl3-OH

Tl4-E
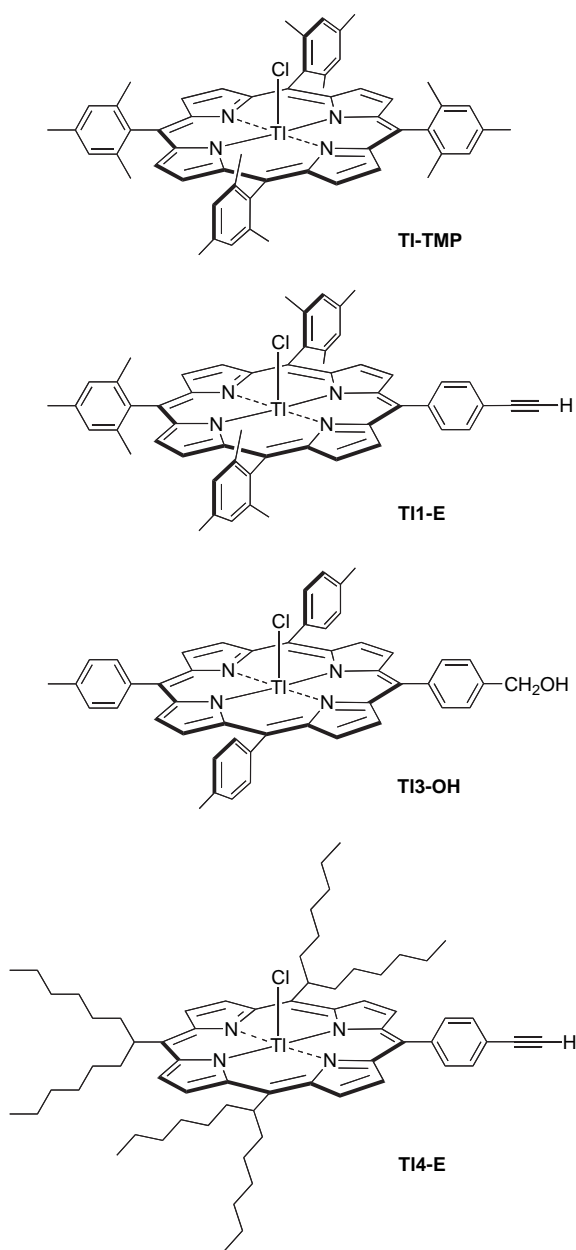
Chart 2.

metalloporphyrins.[43] Thallium complexation causes a bathochromic shift of the B band (∼16 nm), and the Q bands appear at around 568 and 608 nm. The absorption spectra of thallium(III) complexes of porphyrin monomers prepared herein (**Tl-TMP**, **Tl1-E**, and **Tl3-OH**) are essentially the same as previously reported for the thallium(III) complexes of *meso*-tetraarylporphyrins.[48,49,52] The absorption spectra of the thallium(III) complexes of porphyrin dyads dimers containing biphenyl, terphenyl, quaterphenyl, diphenylethyne, and diphenylbutadiyne linkers are similar to those of the corresponding thallium(III) complexes of the porphyrin monomers. On the other hand, the *p*-phenylene-linked dyad shows a split B band owing to strong electronic coupling between the two porphyrins (Fig. 3).

4. Outlook

Extensive studies in artificial photosynthesis spanning more than 30 years have yielded a very large collection of molecular architectures containing two porphyrins joined via a covalent linker, yet there remains a need for systematically designed sets of dyads and dimers to address key mechanistic questions. One set of architectures prepared herein includes two *meso*-substituted porphyrins joined via an oligo(*p*-phenylene) linker, mesityl groups at the non-linking *meso* positions, and three different combinations of metalation states. The metalation states include Zn(II)/free base for study of excited-state energy-transfer and hole-transfer processes; Tl(III)/Tl(III) for study of ground-state hole-transfer processes; and free base/free base as synthetic intermediates. The oligo(*p*-phenylene) linker, while examined previously in a variety of arrays but not in the systematic set of porphyrin dyads as prepared herein, enables a range of porphyrin/porphyrin distances of separation to be accessed while limiting changes in other molecular parameters. Several arrays with diphenylethyne or diphenylbutadiyne linkers also were prepared.

There are at least three key distinctions between the oligo(*p*-phenylene) linkers and the linkers containing one or more ethyne units (i.e., diphenylethyne or diphenylbutadiyne). First, the latter are more flexible than the former. The greater flexibility is expected on first principles, is predicted by calculations, and has been established by NMR spectroscopy of analogous multiporphyrin arrays.[63] The greater flexibility stems from the sp-hybridization of the ethyne carbon atoms versus the sp^2-hybridization of the carbon atoms in the aryl units. In other words, the diphenylethyne and diphenylbutadiyne linkers are more prone to bending (at the ethyne carbons) than are the oligo(*p*-phenylene) linkers. Second, the ethyne-containing linkers have a lower energy barrier to rotation about the linker axis versus oligo(*p*-phenylene) linkers owing to the cylindrical symmetry of the ethyne bond. Third, the ethyne-containing linkers generally have smaller HOMO/LUMO gaps than those of the oligo(*p*-phenylene) linkers (although the HOMO/LUMO gaps of the quaterphenyl and diphenylethyne linkers are comparable).[16] Accordingly, arrays of nominally identical distances of separation of the porphyrin centers may exhibit different rates of key processes (excited-state energy transfer and hole transfer; ground-state hole transfer) owing to the distinct physical properties of the two classes of linkers.

5. Experimental

5.1. General methods

^{1}H NMR spectra (300 MHz) and ^{13}C NMR spectra (75 MHz) were collected in CDCl$_3$ or toluene-d_8. Absorption and fluorescence spectra were collected in CH$_2$Cl$_2$ at room temperature unless noted otherwise. Laser-desorption mass spectra of porphyrins were obtained via matrix-assisted laser desorption ionization mass spectrometry (MALDI-MS) using a matrix of 1,4-bis(5-phenyloxazol-2-yl)benzene.[64] Electrospray ionization mass spectrometry (ESIMS) data are reported for the molecule ion or protonated molecule ion. Analytical-scale size-exclusion chromatography (SEC) and preparative-scale SEC (Bio–Beads SX-1, toluene) were carried out as described previously.[36,42,55] Analytical-scale SEC was performed using three columns (100 Å, 500 Å, and 1000 Å; Polymer Laboratories, PLgel GPC) in series eluting with THF at a flow rate of 0.8 mL/min. Neutral alumina (activity grade I) was obtained from commercial suppliers and used as received.

5.2. Solvents

CHCl$_3$ contained 0.8% ethanol. Toluene, DMF, and triethylamine for the Pd-mediated coupling reactions (Suzuki or Sonogashira couplings) were used as obtained from commercial sources without further purification. The solvent mixture of toluene/DMF/water (for Suzuki coupling) or toluene/triethylamine mixture (for
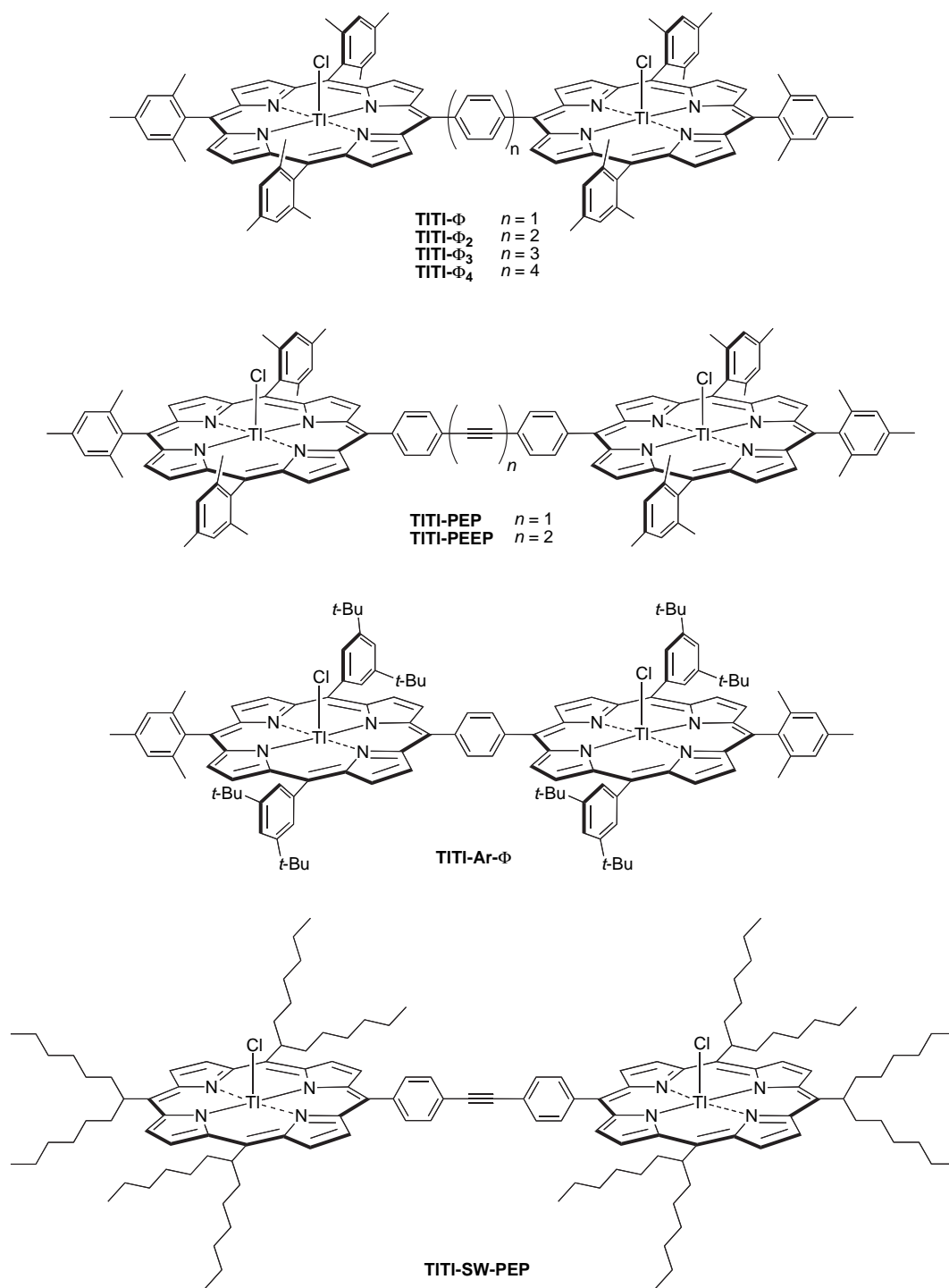
TITI-Φ   *n* = 1
TITI-Φ₂ *n* = 2
TITI-Φ₃ *n* = 3
TITI-Φ₄ *n* = 4

TITI-PEP   *n* = 1
TITI-PEEP *n* = 2

TITI-Ar-Φ

TITI-SW-PEP

Chart 3.

Sonogashira coupling) was freeze/pump/thawed three times under argon prior to use. The Pd-mediated coupling reactions were carried out under anaerobic conditions with the use of standard Schlenk-line techniques.

5.3. Non-commercial compounds

The biphenyl building blocks 4′-bromobiphenyl-4-carboxaldehyde (**I-Br**)[37] and 4′-(4,4,5,5-tetramethyl-1,3,2-dioxaborolan-2-yl)biphenyl-4-carboxaldehyde (**I-B**)[38] the porphyrins *meso*-tetramesitylporphyrin (**Fb-TMP**),[35] zinc(II)-*meso*-

tetramesitylporphyrin (**Zn-TMP**),[62] 5,10,15-trimesityl-20-(4-iodophenyl)porphyrin (**Fb1-I**),[34] zinc(II)-20-(4-iodophenyl)-5,10,15-trimesitylporphyrin (**Zn1-I**),[36] 5-(4-ethynylphenyl)-10,15,20-trimesitylporphyrin (**Fb1-E**),[34] 5-[4-(hydroxymethyl)phenyl]-10,15,20-tri-*p*-tolylporphyrin (**Fb3-OH**),[53] 5-(4-ethynylphenyl)-10,15,20-tris(tridec-7-yl)porphyrin (**Fb4-E**),[39] and 5-(4-iodophenyl)-10,15,20-tris(tridec-7-yl)porphyrin (**Fb4-I**)[39] and the porphyrin dimers 1,4-bis(5,10,15-trimesitylporphin-20-yl)benzene (**FbFbΦ**; *compound* **Fb₂Φ** in Ref. 24),[24] 1,4-bis[5,15-(3,5-di-*tert*-butylphenyl)-10-mesitylporphin-20-yl]benzene (**FbFb-Ar-Φ**; *compound* **12** in Ref. 30),[30] 1,2-bis[4-(5,10,15-trimesitylporphin-20-yl)
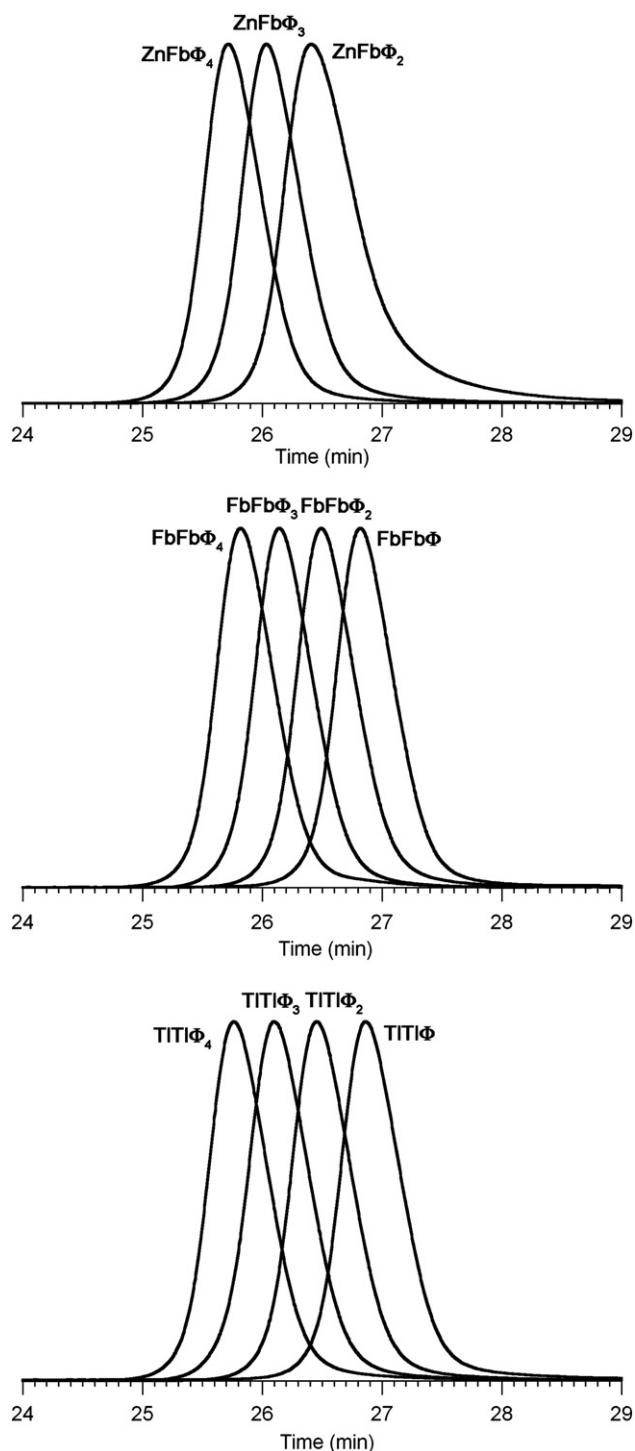
Figure 1. Analytical SEC traces of the three series of oligo(*p*-phenylene)-linked porphyrin dimers and dyads.

Table 3
Analytical SEC retention times of porphyrin dimers and dyads[a]

Compound	Retention time (min)
ZnFbΦ₂	26.41
ZnFbΦ₃	26.04
ZnFbΦ₄	25.72
FbFbΦ	26.92
FbFbΦ₂	26.49
FbFbΦ₃	26.14
FbFbΦ₄	25.82
TlTlΦ	26.86
TlTlΦ₂	26.46
TlTlΦ₃	26.10
TlTlΦ₄	25.76

[a] Data were obtained upon chromatography with three columns (100 Å, 500 Å, and 1000 Å) in series and a flow rate of 0.8 mL/min (THF). The void volume corresponded to ~2.8 min.

trimesitylporphyrin (**Zn1-I**, 93.0 mg, 100 μmol), bis(pinacolato) diboron (76.2 mg, 300 μmol), 1,1′-bis(diphenylphosphino)ferrocene-palladium(II)dichloride dichloromethane adduct [Pd(dppf) Cl₂] (4.9 mg, 6.0 μmol), and potassium acetate (88.3 mg, 0.900 mmol) were weighed into a 25-mL Schlenk flask, which was then pump-purged three times with argon. DMF (10 mL, bubbled through argon for 1 h) was added and the reaction mixture was stirred at 100 °C for 60 h. Standard workup including chromatography [silica, hexanes/CH₂Cl₂/triethylamine (66:33:1)] gave a purple solid (74.1 mg, 78%): ^{1}H NMR (CDCl₃) δ 1.50 (s, 12H), 1.84 (s, 12H), 1.85 (s, 6H), 2.63 (s, 6H+3H), 7.27 (s, 6H), 8.14–8.27 (m, 4H), 8.67–8.72 (m, 4H), 8.74 (d, J=4.7 Hz, 2H), 8.84 (d, J=4.7 Hz, 2H); MALDI-MS obsd 928.9; ESI-HRMS obsd 929.3924 (M+H)$^+$ corresponds to 928.3851 (M), calcd 928.3866 (C₅₉H₅₇BN₄O₂Zn); λ_{abs} (relative intensity) 423 (1.00), 550 (0.05) nm; λ_{em} (λ_{ex}=423 nm) 599, 648 nm.

*5.4.2. 5,10,15-Trimesityl-20-[4′-(4,4,5,5-tetramethyl-1,3,2-dioxaborolan-2-yl)biphen-4-yl]porphyrin (**Fb2-B**).* Following a standard procedure for the synthesis of A₃B-porphyrins via mixed condensations,[34,35] a solution of 4′-(4,4,5,5-tetramethyl-1,3,2-dioxaborolan-2-yl)biphenyl-4-carboxaldehyde (**I-B**, 462 mg, 1.50 mmol, 2.5 mM), mesitaldehyde (667 mg, 4.50 mmol, 7.5 mM), and pyrrole (403 mg, 6.00 mmol, 10 mM) in chloroform (600 mL) was treated with BF₃·O(Et)₂ (222 μL, 1.80 mmol, 3.0 mM) at room temperature for 1 h. After the addition of DDQ (1.02 g, 4.50 mmol), the reaction mixture was stirred at room temperature for 1 h, whereupon triethylamine (0.5 mL) was added. The reaction mixture was concentrated to dryness. The residue was chromatographed [silica, CH₂Cl₂] to give a mixture of porphyrins. The crude porphyrin mixture was subjected to further chromatography [silica, hexanes/CH₂Cl₂ (2:1)]; the second fraction gave the title compound as a purple solid (115 mg, 8%): ^{1}H NMR (CDCl₃) δ −2.57 to −2.52 (br, 2H), 1.42 (s, 12H), 1.85 (s, 6H+12H), 2.62 (s, 3H+6H), 7.28 (s, 6H), 7.94 (d, J=8.1 Hz, 2H), 8.00 (d, J=8.1 Hz, 2H), 8.04 (d, J=8.1 Hz, 2H), 8.27 (d, J=8.1 Hz, 2H), 8.60–8.66 (m, 4H), 8.69 (d, J=4.7 Hz, 2H), 8.85 (d, J=4.7 Hz, 2H); MALDI-MS obsd 942.4 [based on the most abundant (100%) signal]; ESI-HRMS obsd 942.5142, calcd 942.5153 [(M+H)$^+$, M=C₆₅H₆₃BN₄O₂, based on the smallest isotopic (^{10}B) signal]; λ_{abs} (relative intensity) 421 (1.00), 516 (0.05), 549 (0.02), 592 (0.01) nm; λ_{em} (λ_{ex}=421 nm) 653, 723 nm.

*5.4.3. 20-[4′-Bromobiphen-4-yl]-5,10,15-trimesitylporphyrin (**Fb2-Br**).* Following a standard procedure for the synthesis of A₃B-porphyrins via mixed-aldehyde condensations,[34,35] a solution of 4′-bromobiphenyl-4-carboxaldehyde (**I-Br**, 653 mg, 2.50 mmol, 2.5 mM), mesitaldehyde (1.11 g, 7.50 mmol, 7.5 mM), and pyrrole (671 mg, 10.0 mmol, 10 mM) in chloroform (1 L) was treated with BF₃·O(Et)₂ (370 μL, 3.00 mmol, 3.0 mM) at room temperature for 1 h. After the addition of DDQ (1.70 g, 7.50 mmol), the reaction mixture was stirred at room temperature for 1 h, whereupon

phenyl]ethyne (**FbFb-PEP**; *compound* **Fb₂U** in Ref. 54),[54] and 1,4-bis[4-(5,10,15-trimesitylporphin-20-yl)phenyl]buta-1,3-diyne (**FbFb-PEEP**; *compound* **5** in Ref. 41)[41] were prepared following literature procedures.

5.4. Synthesis of porphyrin building blocks

*5.4.1. Zinc(II) 5,10,15-trimesityl-20-[4-(4,4,5,5-tetramethyl-1,3,2-dioxaborolan-2-yl) phenyl]porphyrin (**Zn1-B**).* Following a standard procedure,[31] samples of zinc(II)-20-(4-iodophenyl)-5,10,15-

triethylamine (0.5 mL) was added. The reaction mixture was concentrated to dryness. The residue was chromatographed [silica, CH_2Cl_2] to give a mixture of porphyrins. The crude porphyrin mixture was subjected to further chromatography [silica, hexanes/CH_2Cl_2 (2:1)]; the second fraction gave the title compound as a purple solid (287 mg, 13%): ^1H NMR (CDCl$_3$) δ −2.58 to −2.53 (br, 2H), 1.85 (s, 6H+12H), 2.62 (s, 3H+6H), 7.28 (s, 6H),

Fb-TMP

Zn-TMP

Tl-TMP

Figure 2. ^{13}C NMR spectra of **Fb-TMP** (in toluene-d_8), **Zn-TMP** (in toluene-d_8), and, **Tl-TMP** (in CDCl$_3$). The atom labeling of the *meso*-tetramesitylporphyrin (M=H, H; Zn; or ClTl) macrocycle is shown at top.

7.71 (d, J=8.5 Hz, 2H), 7.79 (d, J=8.5 Hz, 2H), 7.93 (d, J=8.5 Hz, 2H), 8.27 (d, J=8.5 Hz, 2H), 8.61–8.65 (m, 4H), 8.69 (d, J=4.7 Hz, 2H), 8.83 (d, J=4.7 Hz, 2H); MALDI-MS obsd 895.1; ESI-HRMS obsd 895.3374 (M+H)$^+$ corresponds to 894.3301 (M), calcd 894.3297 (C$_{59}$H$_{51}$BrN$_4$); λ_{abs} (relative intensity) 421 (1.00), 516 (0.04), 548 (0.02), 593 (0.01) nm; λ_{em} (λ_{ex}=421 nm) 653, 724 nm.

5.4.4. Zinc(II) 20-(4′-bromobiphenyl-4-yl)-5,10,15-trimesitylporphyrin (Zn2-Br). A solution of **Fb2-Br** (89.6 mg, 100 μmol) in CH_2Cl_2 (20 mL) was treated with a solution of Zn(OAc)$_2$·2H$_2$O (439 mg, 2.00 mmol) in methanol (2 mL), and the reaction mixture was stirred at room temperature for 2 h. Standard workup including chromatography [silica, hexanes/CH_2Cl_2 (2:1)] gave a purple solid (69.8 mg, 73%): ^1H NMR (CDCl$_3$) δ 1.84 (s, 6H+12H), 2.63 (s, 3H+6H), 7.27 (s, 6H), 7.71 (d, J=8.5 Hz, 2H), 7.80 (d, J=8.5 Hz, 2H), 7.93 (d, J=8.1 Hz, 2H), 8.29 (d, J=8.1 Hz, 2H), 8.68–8.73 (m, 4H), 8.77 (d, J=4.7 Hz, 2H), 8.91 (d, J=4.7 Hz, 2H); MALDI-MS obsd 957.1; ESI-HRMS obsd 956.2427 (M)$^+$ corresponds to 956.2432 (M), calcd 956.2432 (C$_{59}$H$_{49}$BrN$_4$Zn); λ_{abs} (relative intensity) 423 (1.00), 550 (0.04) nm; λ_{em} (λ_{ex}=423 nm) 597, 647 nm.

5.5. Synthesis of ZnFb porphyrin dyads

5.5.1. 4-(Zinc(II) 5,10,15-trimesitylporphin-20-yl)-4′-(5,10,15-trimesitylporphin-20-yl)-biphenyl (ZnFbΦ$_2$). Following a standard procedure for Suzuki coupling of porphyrins,[31] samples of **Zn1-B** (46.5 mg, 50.0 μmol), 5,10,15-trimesityl-20-(4-iodophenyl)porphyrin (**Fb1-I**, 43.3 mg, 50.0 μmol), Pd(dppf)Cl$_2$ (12.2 mg, 15.0 μmol), and potassium acetate (73.6 mg, 0.750 mmol) were weighed into a 25-mL Schlenk flask, which was then pump-purged three times with argon. Toluene/DMF/H$_2$O (10:5:1, 10 mL, freeze/pump/thawed three times under argon) was added, and the reaction mixture was stirred at 100 °C for 16 h. Toluene (25 mL) and H$_2$O (25 mL) were added to the reaction mixture. The organic phase was extracted, dried (Na$_2$SO$_4$), and filtered. The filtrate was concentrated to dryness. The residue was purified by preparative SEC followed by adsorption chromatography [the crude compound was dissolved in a minimal amount of toluene, loaded on silica, and eluted with hexanes/CH_2Cl_2/triethylamine (66:33:1)] to give a purple solid (26.5 mg, 34%): ^1H NMR (toluene-d_8) δ −1.78 to −1.73 (br, 2H), 1.87 (s, 6H), 1.99 (s, 6H+12H), 2.06 (s, 12H), 2.47 (s, 3H), 2.51 (s, 3H+6H), 2.53 (s, 6H), 7.15 (s, 2H), 7.20 (s, 2H+4H), 7.25 (s, 4H), 8.01–8.10 (m, 4H), 8.22 (d, J=8.1 Hz, 2H), 8.39 (d, J=8.1 Hz, 2H), 8.74–8.81 (m, 4H), 8.88 (d, J=4.7 Hz, 2H), 8.89–8.93 (m, 4H), 8.99 (d, J=4.7 Hz, 2H), 9.06 (d, J=4.7 Hz, 2H), 9.18 (d, J=4.7 Hz, 2H); MALDI-MS obsd 1541.0; ESI-HRMS obsd 1541.6844 (M+H)$^+$ corresponds to 1540.6771 (M), calcd 1540.6736 (C$_{106}$H$_{92}$N$_8$Zn); λ_{abs} (relative intensity) 426 (1.00), 516 (0.03), 550 (0.04), 592 (0.01) nm; λ_{em} (λ_{ex}=426 nm) 653, 724 nm.

5.5.2. 4-(Zinc(II) 5,10,15-trimesitylporphin-20-yl)-4″-(5,10,15-trimesitylporphin-20-yl)terphenyl (ZnFbΦ$_3$). Following the general procedure described in the Section 5.5.1, samples of **Zn1-B** (46.5 mg, 50.0 μmol), **Fb2-Br** (44.8 mg, 50.0 μmol), Pd(dppf)Cl$_2$ (12.2 mg, 15.0 μmol), and potassium acetate (73.6 mg, 0.750 mmol) were treated in toluene/DMF/H$_2$O (10:5:1, 10 mL) at 100 °C for 16 h. Standard workup including chromatography [preparative SEC, toluene; silica, hexanes/CH_2Cl_2/triethylamine (66:33:1)] gave a purple solid (47.0 mg, 58%): ^1H NMR (toluene-d_8) δ −1.80 to −1.76 (br, 2H), 1.86 (s, 6H), 1.98 (s, 12H), 1.99 (s, 6H), 2.06 (s, 12H), 2.47 (s, 3H), 2.51 (s, 3H+6H), 2.54 (s, 6H), 7.14 (s, 2H), 7.20 (s, 2H+4H), 7.25 (s, 4H), 7.89–8.02 (m, 8H), 8.18 (d, J=8.1 Hz, 2H), 8.35 (d, J=8.1 Hz, 2H), 8.73–8.80 (m, 4H), 8.85 (d, J=4.7 Hz, 2H), 8.82–8.93 (m, 4H), 8.96 (d, J=4.7 Hz, 2H), 9.00 (d, J=4.7 Hz, 2H), 9.12 (d, J=4.7 Hz, 2H); MALDI-MS obsd 1617.4; ESI-HRMS obsd 1617.7122 (M+H)$^+$ corresponds to 1616.7049 (M), calcd 1616.7049 (C$_{112}$H$_{96}$N$_8$Zn); λ_{abs}
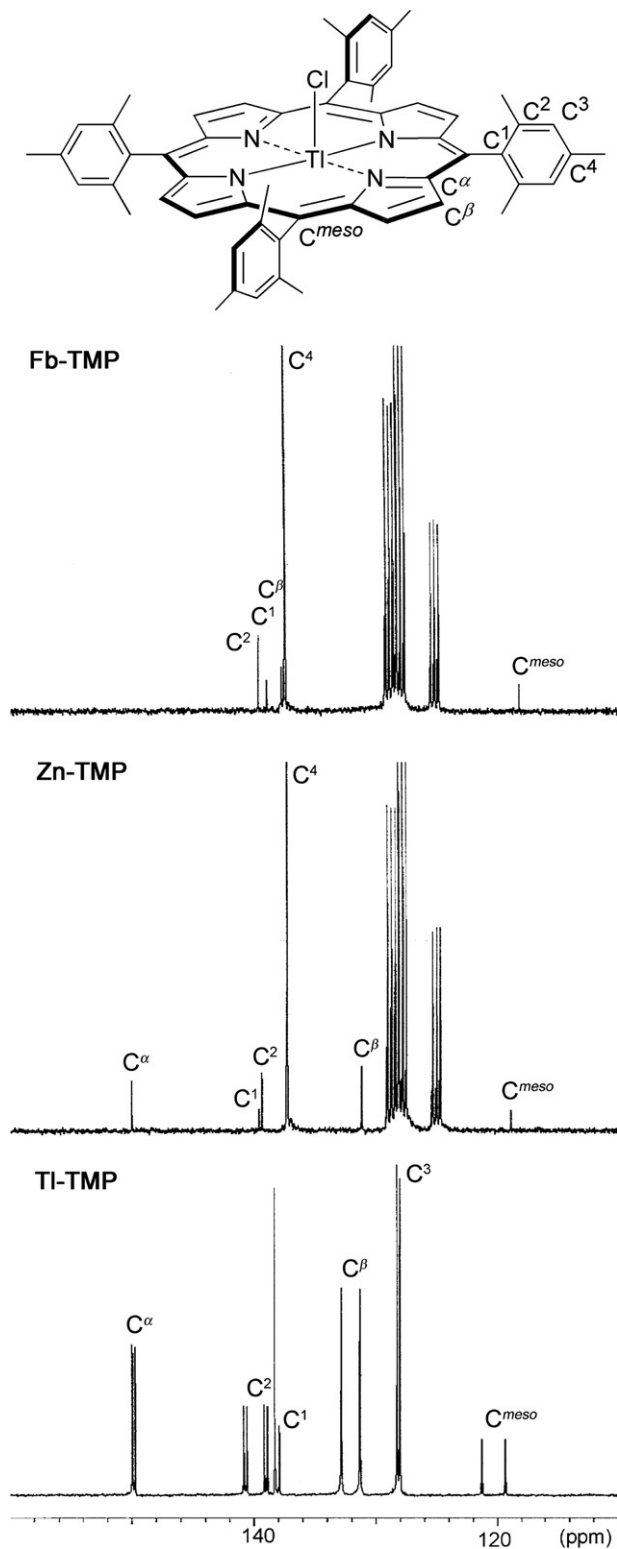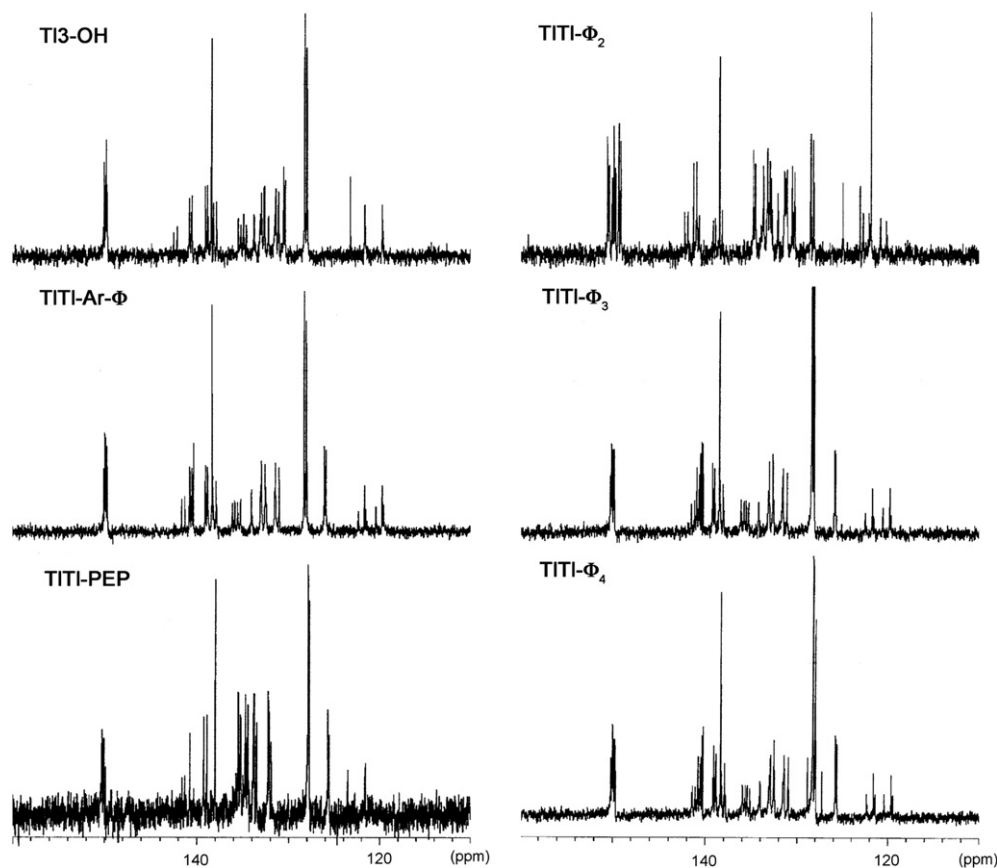
Figure 3. ^{13}C NMR spectra of **Tl-3OH**, **TlTl-Ar-Φ**, **TlTl-PEP**, **TlTl-Φ₂**, **TlTl-Φ₃**, and **TlTl-Φ₄**, (in CDCl₃), typically the result of data acquisition over the course of 12–18 h.

(relative intensity) 425 (1.00), 516 (0.02), 550 (0.04), 592 (0.01) nm; λ_{em} (λ_{ex}=425 nm) 653, 724 nm.

*5.5.3. 4-(Zinc(II) 5,10,15-trimesitylporphin-20-yl)-4″-(5,10,15-tri-mesitylporphin-20-yl)quaterphenyl (**ZnFbΦ₄**).* Following the general procedure described in the Section 5.5.1, samples of **Zn2-Br** (48.0 mg, 50.0 μmol), **Fb2-B** (47.0 mg, 50.0 μmol), Pd(dppf)Cl₂ (12.2 mg, 15.0 μmol), and potassium acetate (73.6 mg, 0.750 mmol)

were treated in toluene/DMF/H₂O (10:5:1, 10 mL) at 100 °C for 16 h. Standard workup including chromatography [preparative SEC, toluene; silica, hexanes/CH₂Cl₂/triethylamine (66:33:1)] gave a purple solid (53.5 mg, 63%): ^{1}H NMR (toluene-d_8) δ −1.80 to −1.76 (br, 2H), 1.86 (s, 6H), 1.98 (s, 6H+12H), 2.05 (s, 12H), 2.47 (s, 3H), 2.50 (s, 3H+6H), 2.53 (s, 6H), 7.15 (s, 2H), 7.20 (s, 2H+4H), 7.24 (s, 4H), 7.78–7.99 (m, 12H), 8.16 (d, J=8.1 Hz, 2H), 8.34 (d, J=8.1 Hz, 2H), 8.74–8.80 (m, 4H), 8.84 (d, J=4.7 Hz, 2H), 8.88–8.92 (m, 4H), 8.95

Table 4
Absorption spectral properties of free base and thallium porphyrins[a]

Compound	B Band	Q Band			
TMP	418 (100)	514 (4.3)	547 (1.2)	590 (1.2)	647 (0.8)
Tl-TMP	434 (100)	529 (sh, 0.8)	567 (3.9)	606 (1.7)	
Tl1-E	437 (100)	529 (sh, 1.3)	569 (4.2)	609 (3.2)	
Fb3-OH	419 (100)	516 (3.9)	552 (2.0)	590 (1.2)	647 (1.0)
Tl3-OH	435 (100)	528 (sh, 1.3)	569 (4.0)	608 (3.0)	
Fb4-E	421 (100)	521 (4.1)	557 (2.6)	600 (1.3)	656 (1.7)
Tl4-E	435 (100)	533 (sh, 0.8)	575 (3.4)	615 (3.0)	
FbFb-Ar-Φ	419 (87), 427 (100)	518 (6.5)	554 (3.9)	592 (2.3)	648 (2.0)
TlTl-Ar-Φ	435 (88), 443 (100)	530 (sh, 1.5)	569 (6.4)	610 (5.0)	
FbFb-Φ	418 (82), 427 (100)	516 (7.4)	551 (3.3)	592 (2.3)	648 (1.7)
TlTl-Φ	433 (81), 443 (100)	528 (sh, 1.3)	568 (639)	609 (3.8)	
FbFb-Φ₂	423 (100)	516 (5.9)	550 (2.6)	591 (1.8)	647 (1.3)
TlTl-Φ₂	439 (100)	528 (sh, 1.1)	568 (5.7)	608 (3.2)	
FbFb-Φ₃	421 (100)	516 (5.1)	550 (2.1)	592 (1.5)	647 (1.1)
TlTl-Φ₃	437 (100)	528 (sh, 1.2)	568 (4.9)	608 (2.7)	
FbFb-Φ₄	421 (100)	516 (5.0)	549 (2.1)	593 (1.5)	647 (1.0)
TlTl-Φ₄	437 (100)	528 (sh, 0.9)	568 (4.4)	608 (2.4)	
FbFb-PEP	424 (100)	516 (5.4)	551 (2.5)	592 (1.7)	647 (1.2)
TlTl-PEP	439 (100)	527 (sh, 1.0)	568 (5.4)	608 (3.0)	
FbFb-SW-PEP	426 (100)	522 (5.2)	558 (3.6)	600 (1.6)	656 (2.2)
TlTl-SW-PEP	440 (100)	532 (sh, 1.0)	575 (4.9)	615 (4.7)	
FbFb-PEEP	424 (100)	515 (5.6)	550 (2.6)	593 (1.7)	647 (1.3)
TlTl-PEEP	440 (100)	530 (sh, 1.0)	570 (5.4)	610 (3.2)	

[a] At room temperature in dichloromethane. The numbers shown in parentheses are relative intensities in %.
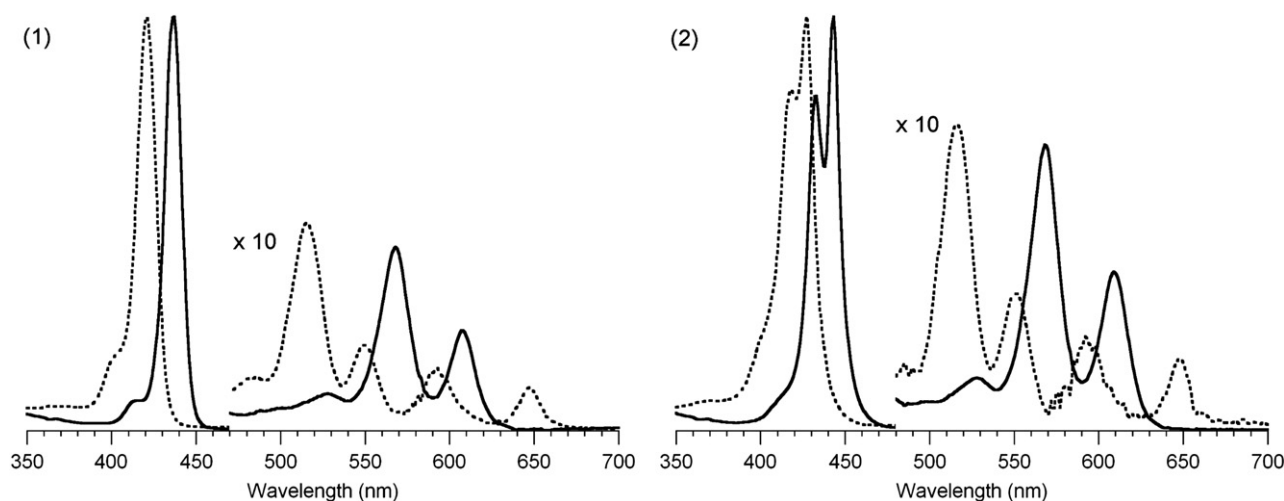
Figure 4. Absorption spectra of thallium(III)porphyrins in CH_2Cl_2 at room temperature. Panel 1: **FbFb-Φ₄** (dashed line), **TlTl-Φ₄** (solid line). Panel 2: **FbFb-Φ** (dashed line), **TlTl-Φ** (solid line).

(d, *J*=4.7 Hz, 2H), 8.99 (d, *J*=4.7 Hz, 2H), 9.12 (d, *J*=4.7 Hz, 2H); MALDI-MS obsd 1693.7; ESI-HRMS obsd 1693.7475 (M+H)$^+$ corresponds to 1962.7402 (M), calcd 1692.7362 ($C_{118}H_{100}N_8Zn$); λ_{abs} (relative intensity) 427 (1.00), 515 (0.03), 556 (0.04), 596 (0.02) nm; λ_{em} (λ_{ex}=423 nm) 653, 723 nm.

5.6. Synthesis of FbFb porphyrin dimers

*5.6.1. 4,4′-Bis(5,10,15-trimesitylporphin-20-yl)biphenyl (**FbFbΦ₂**).* A solution of **ZnFbΦ₂** (23.1 mg, 15.0 µmol) in CH_2Cl_2 (3 mL) was treated with TFA (110 µL, 1.50 mmol) for 2 h. Standard workup including chromatography [silica, hexanes/CH_2Cl_2 (2:1)] gave a purple solid (21.2 mg, 95%): ^{1}H NMR (toluene-d_8) δ −1.83 to −1.77 (br, 4H), 1.82 (s, 12H), 1.94 (s, 24H), 2.42 (s, 6H), 2.46 (s, 12H), 7.10 (s, 4H), 7.16 (s, 8H), 7.96 (AA′BB′, 4H), 8.17 (AA′BB′, 4H), 8.71 (d, *J*=4.8 Hz, 4H), 8.74 (d, *J*=4.8 Hz, 4H), 8.83 (d, *J*=4.8 Hz, 4H), 9.00 (d, *J*=4.8 Hz, 4H); MALDI-MS obsd 1476.5; ESI-HRMS obsd 1479.7665 (M+H)$^+$ corresponds to 1478.7592 (M), calcd 1478.7601 ($C_{106}H_{94}N_8$); λ_{abs} (relative intensity) 423 (1.00), 516 (0.06), 550 (0.03), 591 (0.02), 647 (0.01) nm; λ_{em} (λ_{ex}=423 nm) 651, 721 nm.

*5.6.2. 4,4″-Bis(5,10,15-trimesitylporphin-20-yl)terphenyl (**FbFbΦ₃**).* A solution of **ZnFbΦ₃** (32.4 mg, 20.0 µmol) in CH_2Cl_2 (4 mL) was treated with TFA (0.15 mL, 2.0 mmol) for 2 h. Standard workup including chromatography [silica, hexanes/CH_2Cl_2 (1:1)] gave a purple solid (24.0 mg, 77%): ^{1}H NMR (CDCl₃) δ −2.54 to −2.48 (br, 4H), 1.88 (s, 12H+24H), 2.63 (s, 6H), 2.64 (s, 12H), 7.28 (s, 4H), 7.30 (s, 8H), 8.12 (AA′BB′, 4H), 8.14−8.18 (m, 4H), 8.35 (AA′BB′, 4H), 8.62−8.68 (m, 8H), 8.73 (d, *J*=4.8 Hz, 4H), 8.92 (d, *J*=4.8 Hz, 4H); MALDI-MS obsd 1552.7; ESI-HRMS obsd 1555.7948 (M+H)$^+$ corresponds to 1554.7855 (M), calcd 1554.7914 ($C_{112}H_{98}N_8$); λ_{abs} (relative intensity) 421 (1.00), 516 (0.05), 550 (0.02), 592 (0.02), 647 (0.01) nm; λ_{em} (λ_{ex}=421 nm) 652, 721 nm.

*5.6.3. 4,4‴-Bis(5,10,15-trimesitylporphin-20-yl)quaterphenyl (**FbFbΦ₄**).* A solution of **ZnFbΦ₄** (33.9 mg, 20.0 µmol) in CH_2Cl_2 (4 mL) was treated with TFA (0.15 mL, 2.0 mmol) for 2 h. Standard workup including chromatography [silica, hexanes/toluene (1:1)] gave a purple solid (22.8 mg, 70%): ^{1}H NMR (toluene-d_8) δ −1.81 to −1.75 (br, 4H), 1.86 (s, 12H), 1.97 (s, 24H), 2.47 (s, 6H), 2.50 (s, 12H), 7.15 (s, 4H), 7.20 (s, 8H), 7.80 (AA′BB′, 4H), 7.87 (AA′BB′, 4H), 7.90 (AA′BB′, 4H), 8.16 (AA′BB′, 4H), 8.75 (d, *J*=4.8 Hz, 4H), 8.78 (d, *J*=4.8 Hz, 4H), 8.84 (d, *J*=4.8 Hz, 4H), 8.98 (d, *J*=4.8 Hz, 4H); MALDI-MS obsd 1628.4; ESI-HRMS obsd 1631.8279 (M+H)$^+$ corresponds to 1630.8206 (M), calcd 1630.8227 ($C_{118}H_{102}N_8$); λ_{abs} (relative

intensity) 421 (1.00), 516 (0.05), 549 (0.02), 593 (0.01), 647 (0.01) nm; λ_{em} (λ_{ex}=421 nm) 652, 720 nm.

*5.6.4. 1,2-Bis[4-[5,10,15-tris(tridec-7-yl)porphin-20-yl]phenyl]ethyne (**FbFb-SW-PEP**).* Following a copper-free procedure for Sonogashira coupling of porphyrins,[41,42] samples of 5-(4-ethynylphenyl)-10,15,20-tris(tridec-7-yl)porphyrin (**Fb4-E**, 14.4 mg, 15.0 µmol), 5-(4-iodo-phenyl)-10,15,20-tris(tridec-7-yl)porphyrin (**Fb4-I**, 15.9 mg, 15.0 µmol), Pd(dba)₃ (2.1 mg, 2.3 µmol), and P(*o*-tol)₃ (5.5 mg, 18 µmol) were weighed into a 10-mL Schlenk flask, which was then pump-purged three times with argon. Toluene/triethylamine (5:1, 6 mL, freeze/pump/thawed three times under argon) was added, and the reaction mixture was stirred at 40 °C for 4.5 h (whereupon analytical SEC showed the completion of the reaction). The crude mixture was concentrated to dryness, and passed through silica [silica, hexanes/CH_2Cl_2 (5:1)] to remove palladiums species and monomeric porphyrins. The residue was purified by preparative SEC followed by adsorption chromatography [silica, hexanes/CH_2Cl_2 (5:1)] to give a purple solid (13.6 mg, 48%): ^{1}H NMR (CDCl₃) δ −2.48 to −2.40 (br, 4H), 0.69−0.80 (m, 36H), 1.03−1.44 (m, 96H), 2.68−2.82 (m, 12H), 2.87−3.01 (m, 12H), 5.08−5.24 (m, 6H), 8.07 (AA′BB′, 2H), 8.25 (AA′BB′, 2H), 8.80−8.91 (m, 4H), 9.44−9.78 (m, 12H); MALDI-MS obsd 1885.8; ESI-HRMS obsd 1888.5165 (M+H)$^+$ corresponds to 1887.5092 (M), calcd 1887.5113 ($C_{132}H_{109}N_8$); λ_{abs} (relative intensity) 426 (100), 522 (5.2), 558 (3.6), 600 (1.6), 656 (2.2) nm.

5.7. Synthesis of chlorothallium(III) porphyrins

CAUTION: Thallium is a toxic substance, is accumulated through the skin and mucous membranes, and should be handled with appropriate care.[65]

*5.7.1. Chloro(tetramesitylporphinato)thallium(III) (**Tl-TMP**).* A solution of *meso*-tetramesitylporphyrin (**Fb-TMP**, 23.5 mg, 30.0 µmol) in DMF (3 mL) was treated with TlCl₃·(H₂O)₄ (93 mg, 0.30 mmol) at 150 °C for 2 h. The reaction mixture was concentrated to dryness under reduced pressure. The resulting residue was dissolved in CH_2Cl_2 (30 mL) and washed with saturated aqueous NaCl. The organic layer was separated, dried (Na₂SO₄), filtered, and concentrated to dryness under reduced pressure. The resulting solid was chromatographed [silica, hexanes/CH_2Cl_2 (2:1)] to give a greenish purple solid (23.1 mg, 75%): ^{1}H NMR (CDCl₃) δ 1.74 (s, 12H), 1.97 (s, 12H), 2.63 (s, 12H), 7.23−7.28 (m, 4H), 7.29−7.34 (m, 4H), 8.82 [d, ^4J (Tl–H)=62.4 Hz, 8H]; ^{13}C NMR (CDCl₃) δ 21.8, 21.9, 22.2, 120.3 [^3J (Tl–C)=146 Hz, C$_{meso}$], 128.0 and 128.2 (C-3), 132.0 [^3J(Tl–C)=

116 Hz, C$_\beta$], 138.0 [^4J(Tl–C)=26 Hz, C-1], 138.3 (C-4), 139.0, and 140.6 [^5J(Tl–C)=19 Hz, C-2], 149.8 [^2J(Tl–C)=19 Hz, C$_\alpha$]; MALDI-MS obsd 1020.5; ESI-HRMS obsd 1021.3688 (M+H)$^+$ corresponds to 1021.3615 (M), calcd 1020.3624 (C$_{56}$H$_{52}$ClN$_4$Tl); λ_{abs} (relative intensity) 434 (100), 529 (sh, 0.8) 567 (3.9), 606 (1.7) nm. Alternatively, a solution of **Fb-TMP** (157 mg, 300 μmol) in CH$_2$Cl$_2$ (36 mL) was treated with a solution of TlCl$_3$·(H$_2$O)$_4$ (1.55 g, 5.00 mmol) in methanol (4 mL) at room temperature for 14 h. Standard workup and recrystallization (diffusion of hexanes into a chloroform solution of the mixture of porphyrins) gave a greenish purple solid (135 mg, 66%). Characterization data (LD-MS, ^{1}H NMR, UV–vis) were identical as described above.

5.7.2. Chloro[5-(4-ethynylphenyl)-10,15,20-trimesitylporphinato] thallium(III) (Tl1-E). A solution of 5-(4-ethynylphenyl)-10,15,20-trimesitylporphyrin (**Fb1-E**, 11.5 mg, 15.0 μmol) in CH$_2$Cl$_2$ (2.25 mL) was treated with a solution of TlCl$_3$·(H$_2$O)$_4$ (93 mg, 0.30 mmol) in methanol (0.75 mL) at room temperature for 30 min. Standard workup including chromatography [silica, hexanes/CH$_2$Cl$_2$ (2:1), then hexanes/CH$_2$Cl$_2$ (1:1)] gave a greenish purple solid (13.6 mg, 90%): ^{1}H NMR (CDCl$_3$) δ 1.74 (s, 6H), 1.76 (s, 3H), 1.93 (s, 3H), 1.95 (s, 6H), 2.64 (s, 3H+6H), 3.33 (s, 1H), 7.24–7.29 (m, 1H+2H), 7.29–7.34 (m, 1H+2H), 7.87 (AA′BB′, 1H), 7.95 (AA′BB′, 1H), 8.05 (AA′BB′, 1H), 8.38 (AA′BB′, 1H), 8.85 [d, ^4J(Tl–H)=62.0 Hz, 2H+2H], 8.89 [dd, ^4J(Tl–H)=62.8 Hz, ^3J(H–H)=4.7 Hz, 2H], 8.94 [dd, ^4J(Tl–H)=64.5 Hz, ^3J(H–H)=4.7 Hz, 2H]; MALDI-MS obsd 1002.4; ESI-HRMS obsd 1003.3209 (M+H)$^+$ corresponds to 1002.3136 (M), calcd 1002.3155 (C$_{55}$H$_{46}$ClN$_4$Tl); λ_{abs} (relative intensity) 437 (100), 529 (sh, 1.3), 569 (4.2), 609 (3.2) nm.

5.7.3. Chloro[5-[4-(hydroxymethyl)phenyl]-10,15,20-tri-p-tolylporphinato]thallium(III) (Tl3-OH). A solution of 5-[4-(hydroxymethyl)phenyl]-10,15,20-tri-*p*-tolylporphyrin (**Fb3-OH**, 27.5 mg, 40.0 μmol) in CH$_2$Cl$_2$ (6 mL) was treated with a solution of TlCl$_3$·(H$_2$O)$_4$ (0.25 g, 0.80 mmol) in methanol (2 mL) at room temperature for 48 h. Standard workup including chromatography (silica, CH$_2$Cl$_2$) gave a greenish purple solid (28.7 mg, 78%): ^{1}H NMR (CDCl$_3$) δ 2.01 (t, J=6.0 Hz, 1H), 2.71 (s, 3H+s, 6H), 5.07 (d, J=6.0 Hz, 2H), 7.54 (AA′BB′, 1H+2H), 7.61 (AA′BB′, 1H+2H), 7.75 (AA′BB′, 1H), 7.79 (AA′BB′, 1H), 8.00 (AA′BB′, 1H+2H), 8.12 (AA′BB′, 1H), 8.24 (AA′BB′, 1H+2H), 8.36 (AA′BB′, 1H), 9.02 [dd, ^4J(Tl–H)=65.0 Hz, ^3J(H–H)=4.7 Hz, 2H], 9.07 [d, ^4J(Tl–H)=65.0 Hz, 2H+2H], 9.08 [dd, ^4J(Tl–H)=64.5 Hz, ^3J(H–H)=4.7 Hz, 2H]; MALDI-MS obsd 924.3, calcd 924.2 (C$_{48}$H$_{36}$ClN$_4$OTl); ESI-HRMS obsd 887.2600, calcd 887.2607 [(M–Cl)$^+$, M=C$_{48}$H$_{36}$N$_4$OTl]; λ_{abs} (relative intensity) 435 (100), 528 (sh, 2.3), 569 (4.0), 608 (3.0) nm.

5.7.4. Chloro[5-(4-ethynylphenyl)-10,15,20-tris(tridec-7-yl)porphinato]thallium(III) (Tl4-E). A solution of **Fb4-E** (5.7 mg, 6.0 μmol) in CH$_2$Cl$_2$ (2 mL) was treated with a solution of TlCl$_3$·(H$_2$O)$_4$ (93 mg, 0.30 mmol) in methanol (0.5 mL) at room temperature for 2 h. Standard workup including chromatography [silica, hexanes/CH$_2$Cl$_2$ (5:1)] gave a greenish purple solid (4.6 mg, 63%): ^{1}H NMR (CDCl$_3$) δ 0.60–0.80 (m, 18H), 0.98–1.45 (m, 48H), 2.68–3.12 (m, 12H), 3.34 (s, 1H), 5.20–5.41 (m, 3H), 7.80–7.90 (m, 1H), 7.91–8.07 (m, 2H), 8.30–8.42 (m, 1H), 8.95 [d, ^4J(Tl–H)=63.2 Hz, 2H], 9.53–10.08 (m, 6H); MALDI-MS obsd 1193.7; ESI-HRMS obsd 1195.6973 (M+H)$^+$ corresponds to 1194.6900 (M), calcd 1194.6911 (C$_{67}$H$_{94}$ClN$_4$Tl); λ_{abs} (relative intensity) 435 (100), 533 (sh, 0.8), 573 (3.4), 615 (3.0) nm.

5.8. Metalation of FbFb porphyrin dimers to give the bis (thallium) complexes

5.8.1. 1,4-Bis(chlorothallium(III) 5,10,15-trimesitylporphinato-20-yl) benzene (TlTl-Φ). A solution of **FbFb-Φ** (21.0 mg, 15.0 μmol) in

CH$_2$Cl$_2$ (13.5 mL) was treated with a solution of TlCl$_3$·(H$_2$O)$_4$ (233 mg, 0.750 mmol) in methanol (1.5 mL) at room temperature for 2 h. Standard workup including chromatography [silica, hexanes/CH$_2$Cl$_2$ (1:1)] gave a greenish purple solid (22.5 mg, 80%): ^{1}H NMR (CDCl$_3$) δ 1.81 (s, 6H), 1.83 (s, 12H), 1.98 (s, 6H), 2.03 (s, 12H), 2.65 (s, 6H), 2.68 (s, 12H), 7.28–7.31 (m, 2H), 7.31–7.36 (m, 2H+4H), 7.36–7.40 (m, 4H), 8.51 (s, 1H), 8.57 (d, J=8.4 Hz, 1H), 8.81 (d, J=8.4 Hz, 1H, overlapped), 8.88 (s, 1H), 8.90 [d, ^4J(Tl–H)=62.0 Hz, 4H+4H], 9.08 [dd, ^4J(Tl–H)=62.9 Hz, ^3J(H–H)=4.4 Hz, 4H], 9.42 [dd, ^4J(Tl–H)=64.5 Hz, ^3J(H–H)=4.4 Hz, 4H]; MALDI-MS obsd 1879.0; ESI-HRMS obsd 1879.5902 (M+H)$^+$ corresponds to 1878.5829 (M), calcd 1878.5840 (C$_{100}$H$_{86}$Cl$_2$N$_8$Tl$_2$); λ_{abs} (relative intensity) 433 (81), 443 (100), 528 (sh, 1.3), 568 (6.9), 609 (3.8) nm.

5.8.2. 4,4′-Bis(chlorothallium(III) 5,10,15-trimesitylporphinato-20-yl) biphenyl (TlTl-Φ$_2$). A solution of **FbFb-Φ$_2$** (14.8 mg, 10.0 μmol) in CH$_2$Cl$_2$ (20 mL) was treated with a solution of TlCl$_3$·(H$_2$O)$_4$ (155 mg, 0.500 mmol) in methanol (2 mL) at room temperature for 2 h. Standard workup including chromatography [silica, hexanes/CH$_2$Cl$_2$ (1:2)] gave a greenish purple solid (16.1 mg, 83%): ^{1}H NMR (CDCl$_3$) δ 1.79 (s, 6H+12H), 1.97 (s, 6H), 2.00 (s, 12H), 2.64 (s, 6H), 2.66 (s, 12H), 7.26–7.32 (m, 2H+4H), 7.32–7.38 (m, 2H+4H), 8.33 (s, 2H+2H), 8.41 (d, J=8.1 Hz, 2H), 8.65 (d, J=8.1 Hz, 2H), 8.88 [d, ^4J(Tl–H)=61.6 Hz, 4H+4H], 8.96 [dd, ^4J(Tl–H)=63.4 Hz, ^3J(H–H)=4.4 Hz, 4H], 9.17 [dd, ^4J(Tl–H)=65.4 Hz, ^3J(H–H)=4.4 Hz, 4H]; MALDI-MS obsd 1955.3; ESI-HRMS obsd 1955.6167 (M+H)$^+$ corresponds to 1954.6094 (M), calcd 1954.6153 (C$_{106}$H$_{90}$Cl$_2$N$_8$Tl$_2$); λ_{abs} (relative intensity) 439 (100), 528 (sh, 1.1), 568 (5.7), 608 (3.2) nm.

5.8.3. 4,4″-Bis(chlorothallium(III) 5,10,15-trimesitylporphinato-20-yl)terphenyl (TlTl-Φ$_3$). A solution of **FbFb-Φ$_3$** (15.6 mg, 10.0 μmol) in CH$_2$Cl$_2$ (9 mL) was treated with a solution of TlCl$_3$·(H$_2$O)$_4$ (155 mg, 0.500 mmol) in methanol (1 mL) at room temperature for 14 h. Standard workup including chromatography [silica, hexanes/CH$_2$Cl$_2$ (2:3), then hexanes/CH$_2$Cl$_2$ (1:2)] gave a greenish purple solid (17.0 mg, 84%): ^{1}H NMR (CDCl$_3$) δ 1.78 (s, 6H+12H), 1.96 (s, 6H), 1.99 (s, 12H), 2.65 (s, 6H+12H), 7.26–7.39 (m, 12H), 8.12 (d, J=8.1 Hz, 2H), 8.17 (s, 2H+2H), 8.17–8.27 (m, 12H), 8.57 (d, J=8.1 Hz, 2H), 8.87 [d, ^4J(Tl–H)=61.2 Hz, 4H+4H], 8.94 [dd, ^4J(Tl–H)=63.2 Hz, ^3J(H–H)=4.8 Hz, 4H], 9.12 [dd, ^4J(Tl–H)=64.9 Hz, ^3J(H–H)=4.8 Hz, 4H]; MALDI-MS obsd 2030.5; ESI-HRMS obsd 2031.6491 (M+H)$^+$ corresponds to 2030.6418 (M), calcd 2030.6466 (C$_{112}$H$_{94}$Cl$_2$N$_8$Tl$_2$); λ_{abs} (relative intensity) 437 (100), 528 (sh, 1.2), 568 (4.9), 608 (2.7) nm.

5.8.4. 4,4‴-Bis(chlorothallium(III) 5,10,15-trimesitylporphinato-20-yl)quaterphenyl (TlTl-Φ$_4$). A solution of **FbFb-Φ$_4$** (16.3 mg, 10.0 μmol) in CH$_2$Cl$_2$ (9 mL) was treated with a solution of TlCl$_3$·(H$_2$O)$_4$ (155 mg, 0.500 mmol) in methanol (1 mL) at room temperature for 2 h. Standard workup including chromatography [silica, hexanes/CH$_2$Cl$_2$ (2:1), then hexanes/CH$_2$Cl$_2$ (1:1)] gave a greenish purple solid (16.4 mg, 78%): ^{1}H NMR (CDCl$_3$) δ 1.77 (s, 12H), 1.78 (s, 6H), 1.96 (s, 6H), 1.99 (s, 12H), 2.65 (s, 6H+12H), 7.26–7.31 (m, 2H+4H), 7.31–7.37 (m, 2H+4H), 8.00 (d, J=8.1 Hz, 4H), 8.07 (d, J=8.1 Hz, 2H, overlapped), 8.11 (d, J=8.1 Hz, 4H), 8.16 (d, J=8.1 Hz, 2H), 8.21 (d, J=8.1 Hz, 2H), 8.54 (d, J=8.1 Hz, 2H), 8.86 [d, ^4J(Tl–H)=61.6 Hz, 4H+4H], 8.93 [dd, ^4J(Tl–H)=63.4 Hz, ^3J(H–H)=4.8 Hz, 4H], 9.10 [dd, ^4J(Tl–H)=64.7 Hz, ^3J(H–H)=4.8 Hz, 4H]; MALDI-MS obsd 2106.5; ESI-HRMS obsd 2107.6809 (M+H)$^+$ corresponds to 2106.6736 (M), calcd 2106.6779 (C$_{118}$H$_{98}$Cl$_2$N$_8$Tl$_2$); λ_{abs} (relative intensity) 437 (100), 528 (sh, 0.9), 568 (4.4), 608 (2.4) nm.

5.8.5. 1,4-Bis[chlorothallium(III) 5,15-bis(3,5-di-tert-butylphenyl)-10-trimesitylporphinato-20-yl]benzene (TlTl-Ar-Φ). A solution of **FbFb-Ar-Φ** (16.8 mg, 10.0 μmol) in DMF (2 mL) was treated with TlCl$_3$·(H$_2$O)$_4$ (155 mg, 0.500 mmol) at 150 °C for 2 h. Standard

workup including chromatography [neutral alumina activity I, hexanes/CH_2Cl_2 (2:1)] gave a greenish purple solid (16.2 mg, 75%): ^{1}H NMR ($CDCl_3$) δ 1.57 (s, 36H), 1.62 (s, 36H), 1.83 (s, 6H), 2.00 (s, 6H), 2.66 (s, 6H), 7.29–7.32 (m, 2H), 7.33–7.38 (m, 2H), 7.88 (t, J=1.8 Hz, 4H), 8.08–8.12 (m, 4H), 8.29–8.34 (m, 4H), 8.53 (s, 1H), 8.58 (d, J=8.1 Hz, 1H), 8.79 (d, J=8.1 Hz, 1H), 8.86 (s, 1H, overlapped), 8.97 [dd, [4]J(Tl–H)=62.5 Hz, [3]J(H–H)=4.8 Hz, 4H], 9.13 [dd, [4]J(Tl–H)=64.9 Hz, [3]J(H–H)=4.8 Hz, 4H], 9.29 [dd, [4]J(Tl–H)=65.9 Hz, [3]J(H–H)=4.8 Hz, 4H], 9.50 [dd, [4]J(Tl–H)=63.2 Hz, [3]J(H–H)=4.8 Hz, 4H]; MALDI-MS obsd 2159.0; ESI-HRMS obsd 2159.8979 (M+H)[+] corresponds to 2158.8906 (M), calcd 2158.8970 ($C_{120}H_{126}Cl_2N_8Tl_2$); λ_{abs} (relative intensity) 435 (88), 443 (100), 530 (sh, 1.5), 569 (6.4), 610 (5.0) nm.

*5.8.6. 1,2-Bis[chlorothallium(III) 4-(5,10,15-trimesitylporphinato-20-yl)phenyl]ethyne (**TlTl-PEP**).* A solution of **FbFb-PEP** (15.0 mg, 10.0 μmol) in CH_2Cl_2 (4.5 mL) was treated with a solution of $TlCl_3\cdot(H_2O)_4$ (155 mg, 0.500 mmol) in methanol (0.5 mL) at room temperature for 16 h. Standard workup including chromatography [neutral alumina activity I, hexanes/CH_2Cl_2 (2:1), then hexanes/CH_2Cl_2 (1:2)] gave a greenish purple solid (14.1 mg, 71%): ^{1}H NMR ($CDCl_3$) δ 1.77 (s, 12H), 1.78 (s, 6H), 1.95 (s, 6H), 1.98 (s, 12H), 2.64 (s, 6H), 2.65 (s, 12H), 7.26–7.31 (m, 2H+4H), 7.31–7.37 (m, 6H), 8.06 (AA′BB′, 2H), 8.15 (AA′BB′, 2H), 8.18 (AA′BB′, 2H), 8.50 (AA′BB′, 2H), 8.87 [d, [4]J(Tl–H)=61.6 Hz, 4H+4H], 8.95 [dd, [4]J(Tl–H)=63.1 Hz, [3]J(H–H)=4.8 Hz, 4H], 9.06 [dd, [4]J(Tl–H)=64.9 Hz, [3]J(H–H)=4.8 Hz, 4H]; MALDI-MS obsd 1978.2; ESI-HRMS obsd 1979.6169 (M+H)[+] corresponds to 1978.6096 (M), calcd 1978.6153 ($C_{108}H_{90}Cl_2N_8Tl_2$); λ_{abs} (relative intensity) 439 (100), 527 (sh, 1.0), 568 (5.4), 608 (3.0) nm.

*5.8.7. 1,2-Bis[chlorothallium(III) 4-[5,10,15-tris(tridec-7-yl)porphinato-20-yl]phenyl]ethyne (**TlTl-SW-PEP**).* A solution of **FbFb-SW-PEP** (11.3 mg, 6.00 μmol) in CH_2Cl_2 (5 mL) was treated with a solution of $TlCl_3\cdot(H_2O)_4$ (93 mg, 0.30 mmol) in methanol (1 mL) at room temperature for 2 h. Standard workup including chromatography [silica, hexanes/CH_2Cl_2 (2:1), then hexanes/CH_2Cl_2 (1:1)] gave a greenish purple solid (10.8 mg, 76%): ^{1}H NMR ($CDCl_3$) δ 0.61–0.81 (m, 36H), 1.01–1.47 (m, 96H), 2.72–3.14 (m, 24H), 5.26–5.46 (m, 6H), 8.03–8.22 (m, 6H), 8.45–8.58 (m, 2H), 9.09 [d, [4]J(Tl–H)=64.9 Hz, 4H], 9.62–10.12 (m, 12H); MALDI-MS obsd 2362.7; ESI-HRMS obsd 2364.3664 (M+H)[+] corresponds to 2363.3591 (M), calcd 2363.3665 ($C_{132}H_{186}Cl_2N_8Tl_2$); λ_{abs} (relative intensity) 440 (100), 532 (sh, 1.0), 575 (4.9), 615 (4.7) nm.

*5.8.8. 1,4-Bis[chlorothallium(III) 4-(5,10,15-trimesitylporphinato-20-yl)phenyl]buta-1,3-diyne (**TlTl-PEEP**).* A solution of **FbFb-PEEP** (15.3 mg, 10.0 μmol) in $CHCl_3$ (1.5 mL) was treated with a solution of $TlCl_3\cdot(H_2O)_4$ (62 mg, 0.20 mmol) in methanol (0.5 mL) under reflux for 1.5 h. Standard workup including chromatography [silica, hexanes/CH_2Cl_2 (2:1), then hexanes/CH_2Cl_2 (1:1)] gave a greenish purple solid (13.3 mg, 66%): ^{1}H NMR ($CDCl_3$) δ 1.76 (s, 12H), 1.77 (s, 6H), 1.95 (s, 6H), 1.97 (s, 12H), 2.64 (s, 6H), 2.65 (s, 12H), 7.25–7.31 (m, 2H+4H), 7.31–7.36 (m, 2H+4H), 7.99 (AA′BB′, 2H), 8.07 (AA′BB′, 2H), 8.12 (AA′BB′, 2H), 8.46 (AA′BB′, 2H), 8.85 [d, [4]J(Tl–H)=61.5 Hz, 4H+4H], 8.92 [dd, [4]J(Tl–H)=63.3 Hz, [3]J(H–H)=4.7 Hz, 4H], 9.00 [dd, [4]J(Tl–H)=65.0 Hz, [3]J(H–H)=4.7 Hz, 4H]; MALDI-MS obsd 2001.1; ESI-HRMS obsd 2003.6203 (M+H)[+] corresponds to 2002.6130 (M), calcd 2002.6153 ($C_{110}H_{90}Cl_2N_8Tl_2$); λ_{abs} (relative intensity) 440 (100), 530 (sh, 1.0), 570 (5.4), 610 (3.2) nm.

Acknowledgements

Supplementary data

^{13}C NMR spectra of eight compounds are provided, including seven thallium-containing porphyrin monomers and dimers. Supplementary data associated with this article can be found in the online version at doi:10.1016/j.tet.2010.05.059.

References and notes

1. Maretina, I. A. *Russ. J. Gen. Chem.* **2009**, *79*, 1544–1581.
2. Aratani, N.; Kim, D.; Osuka, A. *Acc. Chem. Res.* **2009**, *42*, 1922–1934.
3. Flamigni, L. *J. Photochem. Photobiol. C: Photochem. Rev.* **2007**, *8*, 191–210.
4. Lo, P.-C.; Leng, X.; Ng, D. K. P. *Coord. Chem. Rev.* **2007**, *251*, 2334–2353.
5. Iengo, E.; Scandola, F.; Alessio, E. *Struct. Bond.* **2006**, *121*, 105–143.
6. Harvey, P. D. In *The Porphyrin Handbook*; Kadish, K. M., Smith, K. M., Guilard, R., Eds.; Academic: San Diego, CA, 2003; Vol. 18, pp 63–250.
7. Holten, D.; Bocian, D. F.; Lindsey, J. S. *Acc. Chem. Res.* **2002**, *35*, 57–69.
8. Aratani, N.; Osuka, A. *Chem. Record* **2003**, *3*, 225–234.
9. Burrell, A. K.; Officer, D. L.; Plieger, P. G.; Reid, D. C. W. *Chem. Rev.* **2001**, *101*, 2751–2796.
10. Gust, D.; Moore, T. A. In *The Porphyrin Handbook*; Kadish, K. M., Smith, K. M., Guilard, R., Eds.; Academic: San Diego, CA, 2000; Vol. 8, pp 153–190.
11. Gribkova, S. E.; Evstigneeva, R. P.; Luzgina, V. N. *Russ. Chem. Rev.* **1993**, *62*, 963–979.
12. Wasielewski, M. R. *Chem. Rev.* **1992**, *92*, 435–461.
13. Wasielewski, M. R. In *Chlorophylls*; Scheer, H., Ed.; CRC: Boca Raton, FL, USA, 1991; pp 269–286.
14. Gust, D.; Moore, T. A. *Adv. Photochem.* **1991**, *16*, 1–65.
15. Song, H.-E.; Kirmaier, C.; Taniguchi, M.; Diers, J. R.; Bocian, D. F.; Lindsey, J. S.; Holten, D. *J. Am. Chem. Soc.* **2008**, *130*, 15636–15648.
16. Song, H.-E.; Taniguchi, M.; Diers, J. R.; Kirmaier, C.; Bocian, D. F.; Lindsey, J. S.; Holten, D. *J. Phys. Chem. B* **2009**, *113*, 16483–16493.
17. Heiler, D.; McLendon, G.; Rogalskyj, P. *J. Am. Chem. Soc.* **1987**, *109*, 604–606.
18. Helms, A.; Heiler, D.; McLendon, G. *J. Am. Chem. Soc.* **1992**, *114*, 6227–6238.
19. Osuka, A.; Ikawa, Y.; Maruyama, K. *Bull. Chem. Soc. Jpn.* **1992**, *65*, 3322–3330.
20. Osuka, A.; Tanabe, N.; Kawabata, S.; Yamazaki, I.; Nishimura, Y. *J. Org. Chem.* **1995**, *60*, 7177–7185.
21. Cho, H. S.; Jeong, D. H.; Yoon, M.-C.; Kim, Y. H.; Kim, Y.-R.; Kim, D.; Jeoung, S. C.; Kim, S. K.; Aratani, N.; Shinmori, H.; Osuka, A. *J. Phys. Chem. A* **2001**, *105*, 4200–4210.
22. Asano, M. S.; Ishizuka, K.; Kaizu, Y. *Mol. Phys.* **2006**, *104*, 1609–1618.
23. (a) Rempel, U.; von Maltzan, B.; von Borczyskowski, C. *Chem. Phys. Lett.* **1995**, *245*, 253–261; (b) Chernook, A.; Shulga, A.; Zenkevich, E.; Rempel, U.; von Borczyskowski, C. *J. Phys. Chem.* **1996**, *100*, 1918–1926.
24. Yang, S. I.; Lammi, R. K.; Seth, J.; Riggs, J. A.; Arai, T.; Kim, D.; Bocian, D. F.; Holten, D.; Lindsey, J. S. *J. Phys. Chem. B* **1998**, *102*, 9426–9436.
25. Lee, S. J.; Mulfort, K. L.; Zuo, X.; Goshe, A. J.; Wesson, P. J.; Nguyen, S. T.; Hupp, J. T.; Tiede, D. M. *J. Am. Chem. Soc.* **2008**, *130*, 836–838.
26. Lee, S. J.; Cho, S.-H.; Mulfort, K. L.; Tiede, D. M.; Hupp, J. T.; Nguyen, S. T. *J. Am. Chem. Soc.* **2008**, *130*, 16828–16829.
27. Cho, S.; Yoon, M.-C.; Kim, C. H.; Aratani, N.; Mori, G.; Joo, T.; Osuka, A.; Kim, D. *J. Phys. Chem. C* **2007**, *111*, 14881–14888.
28. Nagata, T. *Bull. Chem. Soc. Jpn.* **1991**, *64*, 3005–3016.
29. Osuka, A.; Zhang, R.-P.; Maruyama, K.; Ohno, T.; Nozaki, K. *Bull. Chem. Soc. Jpn.* **1993**, *66*, 3773–3782.
30. Yu, L.; Lindsey, J. S. *Tetrahedron* **2001**, *57*, 9285–9298.
31. Hodgkiss, J. M.; Krivokapić, A.; Nocera, D. G. *J. Phys. Chem. B* **2007**, *111*, 8258–8268.
32. Speckbacher, M.; Yu, L.; Lindsey, J. S. *Inorg. Chem.* **2003**, *42*, 4322–4337.
33. Lindsey, J. S. *Acc. Chem. Res.* **2010**, *43*, 300–311.
34. Lindsey, J. S.; Prathapan, S.; Johnson, T. E.; Wagner, R. W. *Tetrahedron* **1994**, *50*, 8941–8968.
35. Lindsey, J. S.; Wagner, R. W. *J. Org. Chem.* **1989**, *54*, 828–836.
36. Wagner, R. W.; Johnson, T. E.; Lindsey, J. S. *J. Am. Chem. Soc.* **1996**, *118*, 11166–11180.
37. van Heerden, P. S.; Bezuidenhoudt, B. C. B.; Ferreira, D. *J. Chem. Soc., Perkin Trans. 1* **1997**, 1141–1146.
38. Chen, H.-B.; Yin, J.; Wang, Y.; Pei, J. *Org. Lett.* **2008**, *10*, 3113–3116.
39. Thamyongkit, P.; Speckbacher, M.; Diers, J. R.; Kee, H. L.; Kirmaier, C.; Holten, D.; Bocian, D. F.; Lindsey, J. S. *J. Org. Chem.* **2004**, *69*, 3700–3710.
40. Thamyongkit, P.; Lindsey, J. S. *J. Org. Chem.* **2004**, *69*, 5796–5799.
41. Wagner, R. W.; Johnson, T. E.; Li, F.; Lindsey, J. S. *J. Org. Chem.* **1995**, *60*, 5266–5273.
42. Wagner, R. W.; Ciringh, Y.; Clausen, C.; Lindsey, J. S. *Chem. Mater.* **1999**, *11*, 2974–2983.

43. Abraham, R. J.; Barnett, G. H.; Smith, K. M. *J. Chem. Soc., Perkin Trans. 1* **1973**, 2142–2148.
44. Abraham, R. J.; Hawkes, G. E.; Smith, K. M. *J. Chem. Soc., Perkin Trans. 2* **1974**, 627–634.
45. Buchler, J. W. In *Porphyrins and Metalloporphyrins*; Smith, K. M., Ed.; Elsevier Scientificlishing, Co.: Amsterdam, 1975; pp 157–231.
46. Krivokapic, A.; Anderson, H. L.; Bourhill, G.; Ives, R.; Clark, S.; McEwan, K. J. *Adv. Mater.* **2001**, *13*, 652–656.
47. Henrick, K.; Matthews, R. W.; Tasker, P. A. *Inorg. Chem.* **1977**, *16*, 3293–3298.
48. Coutsolelos, A. G.; Tsapara, A.; Daphnomili, D.; Ward, D. L. *J. Chem. Soc., Dalton Trans.* **1991**, 3413–3417.
49. Coutsolelos, A. G.; Orfanopoulos, M. *Polyhedron* **1991**, *10*, 885–892.
50. Senge, M. O.; Ruhlandt-Senge, K.; Regli, K. J.; Smith, K. M. *J. Chem. Soc., Dalton Trans.* **1993**, 3519–3538.
51. Sheu, Y.-H.; Hong, T.-N.; Lin, C.-C.; Chen, J.-H.; Wang, S.-S. *Polyhedron* **1997**, *16*, 681–688.
52. Raptopoulou, C.; Daphnomili, D.; Karamalides, A.; Di Vaira, M.; Terzis, A.; Coutsolelos, A. G. *Polyhedron* **2004**, *23*, 1777–1784.
53. Zaidi, S. H. H.; Loewe, R. S.; Clark, B. A.; Jacob, M. J.; Lindsey, J. S. *Org. Process Res. Dev.* **2006**, *10*, 304–314.
54. Li, F.; Gentemann, S.; Kalsbeck, W. A.; Seth, J.; Lindsey, J. S.; Holten, D.; Bocian, D. F. *J. Mater. Chem.* **1997**, *7*, 1245–1262.
55. del Rosario Benites, M.; Johnson, T. E.; Weghorn, S.; Yu, L.; Rao, P. D.; Diers, J. R.; Yang, S. I.; Kirmaier, C.; Bocian, D. F.; HoltenD; Lindsey, J. S. *J. Mater. Chem.* **2002**, *12*, 65–80.
56. Lee, W.-B.; Suen, S.-C.; Jong, T.-T.; Hong, F.-E.; Chen, J.-H.; Lin, H.-J.; Hwang, L.-P. *J. Organomet. Chem.* **1993**, *450*, 63–66.
57. Cheng, T.-W.; Chen, Y.-J.; Hong, F.-E.; Chen, J.-H.; Wang, S.-L.; Hwang, L.-P. *Polyhedron* **1994**, *13*, 403–408.
58. Lu, Y.-Y.; Tung, J.-Y.; Chen, J.-H.; Liao, F.-L.; Wang, S.-L.; Wang, S.-S.; Hwang, L.-P. *Polyhedron* **1999**, *18*, 145–150.
59. Lee, Y.-Y.; Chen, J.-H.; Hsieh, H.-Y.; Liao, F.-L.; Wang, S.-L.; Tung, J.-Y.; Elango, S. *Inorg. Chem. Commun.* **2003**, *6*, 252–258.
60. Tung, J.-Y.; Chen, J.-H.; Liao, F.-L.; Wang, S.-L.; Hwang, L.-P. *Inorg. Chem.* **2000**, *39*, 2120–2124.
61. Medforth, C. J. In *The Porphyrin Handbook*; Kadish, K. M., Smith, K. M., Guilard, R., Eds.; Academic: San Diego, CA, 2000; Vol. 5, pp 1–80.
62. (a) Yang, S. I.; Seth, J.; Strachan, J.-P.; Gentemann, S.; Kim, D.; Holten, D.; Lindsey, J. S.; Bocian, D. F. *J. Porphyrins Phthalocyanines* **1999**, *3*, 117–147; (b) Badger, G. M.; Jones, R. A.; Laslett, R. L. *Aust. J. Chem.* **1964**, *17*, 1028–1035.
63. Bothner-By, A. A.; Dadok, J.; Johnson, T. E.; Lindsey, J. S. *J. Phys. Chem.* **1996**, *100*, 17551–17557.
64. Srinivasan, N.; Haney, C. A.; Lindsey, J. S.; Zhang, W.; Chait, B. T. *J. Porphyrins Phthalocyanines* **1999**, *3*, 283–291.
65. (a) Galvan-Arzate, S.; Santamaria, A. *Toxicol. Lett.* **1998**, *99*, 1–13; (b) Peter, A. L. J.; Viraraghavan, T. *Environ. Int.* **2005**, *31*, 493–501; (c) Mulkey, J. P.; Oehme, F. W. *Vet. Human Toxicol* **1993**, *35*, 445–453; (d) Ibrahim, D.; Froberg, B.; Wolf, A.; Rusyniak, D. E. *Clin. Lab. Med.* **2006**, *26*, 67–97.